Diss. ETH No. 8414

Quasicrystal Structures from the Crystallographic Viewpoint

A dissertation submitted to the
SWISS FEDERAL INSTITUTE OF TECHNOLOGY
ZURICH
for the degree of
Doctor of Natural Sciences

presented by
FRANZ GÄHLER
Dipl. Phys. ETH
born July 26, 1959
citizen of Urnäsch AR

accepted on the recommendation of
Prof. Dr. J. Fröhlich, examiner
Prof. Dr. T.M. Rice, co-examiner

1988

Table of Contents

Zusammenfassung

Quasikristalle sind neuartige Phasen, die in schnell abgekühlten Metall-Legierungen vorkommen. Ihre wichtigste Eigenschaft ist, dass Ihre Fourier-Transformierte aus scharfen Bragg-Peaks besteht, deren Positionen und Intensitäten eine Punktsymmetrie haben, die mit einer dreidimensionalen periodischen Struktur nicht verträglich ist. Die Positionen der Bragg-Peaks eines Quasikristalls können jedoch alle als ganzzahlige Linearkombinationen von endlich vielen fundamentalen Wellenvektoren geschrieben werden; dies legt nahe, diese Strukturen als Schnitt durch eine höherdimensionale, periodische Struktur aufzufassen.

Im ersten Kapitel führen wir eine grosse Klasse diskreter Strukturen ein, deren Beugungsbilder die gewünschten Eigenschaften haben. Wir diskutieren verschiedene Eigenschaften dieser Strukturen. Insbesondere zeigen wir, dass sie fastperiodisch sind, wobei wir eine Definition der Fastperiodizität benützen, die von der durch Bohr für gleichmässig stetige Funktionen gegebenen abgeleitet ist, und die für diskrete Strukturen besonders geeignet ist. Ferner beleuchten wir den Zusammenhang zwischen den Intensitäten im Fourier-Spektrum und dem Konzept des lokalen Isomorphismus.

Als nächstes beginnen wir eine Untersuchung der Kristallographie der Quasikristalle. Kristallographische Konzepte können auf Quasikristalle angewandt werden aufgrund der Beziehung zu einer höherdimensionalen periodischen Struktur. Wir zeigen, wie Konzepte wie Bravais-Klassen, Punktgruppen und Raumgruppen für Quasikristalle definiert werden können, und diskutieren die experimentellen Auswirkungen dieser Symmetrien. In Kapitel zwei geben wir eine vollständige Liste der Bravais-Klassen für diejenigen Punktsymmetrien, die eine höherdimensionale periodische Struktur der Dimension höchstens sechs erfordern. In Kapitel drei leiten wir dann eine vollständige Liste der Punkt- und Raumgruppen her, die in die fünfdimensionalen Bravais-Klassen von Kapitel zwei fallen. Dies sind jene Raumgruppen, deren Punktgruppe im dreidimensionalen Raum (2+1)-R-reduzibel ist. Für jede dieser Raumgruppen geben wir die nicht-primitiven Translationen und die charakteristischen Auslöschungsmuster im Fourier-Spektrum an.

In Kapitel vier sind verschiedene Methoden beschrieben, mit denen quasiperiodische "Tilings" erzeugt werden können. Nach einer kurzen Rekapitulation der klassischen Grid-Projektions-Methode führen wir eine Verallgemeinerung ein, die es erlaubt, Tilings mit beliebiger Punktsymmetrie (im Fourier-Raum) zu erzeugen mit Hilfe von Gittern, deren Dimension die minimale mit der geforderten Punktsymmetrie verträgliche ist. Ferner diskutieren wir eine hierarchische Konstruktionsmethode, die Stampfli eingeführt hat. Wir stellen die Beziehung zu anderen Konstruktionsmethoden her und beweisen damit, dass Stampfli's Tilings tatsächlich quasiperiodisch sind.

In Kapitel fünf beschreiben wir eine detaillierte Modellstruktur für Quasikristalle mit dodekagonaler Symmetrie. Diese Modellstruktur bestimmt alle Atompositionen und wurde von eng verwandten, periodischen Strukturen abgeleitet, die immer zusammen mit der quasikristallinen Phase auftreten. Diese Modellstruktur erlaubt es auch, die zuvor eingeführten kristallographischen Konzepte zu illustrieren. Wir bestimmen sowohl die Punkt- wie auch die Raumgruppe dieser Struktur. Die letztere ist kristallographisch interessant, da sie nicht-symmorph ist und eine Schraubachse sowie einen Satz von Gleitspiegelebenen aufweist. Dann berechnen wir Elektronenbeugungs-Bilder der Modell-Struktur für verschiedene Richtungen des einfallenden Strahls, wobei wir die für Elektronenbeugung wichtigen Mehrfachstreueffekte miteinbeziehen. Die berechneten Bilder zeigen eine gute Übereinstimmung mit experimentellen Resultaten. Wir verifizieren auch, dass die systematischen Auslöschungen mit denen der zuvor bestimmten Raumgruppe identisch sind.

Summary

Quasicrystals are novel phases of rapidly quenched metal alloys. Their main feature is that their Fourier spectrum consists of sharp Bragg peaks whose positions and intensities are invariant under a point symmetry which is incompatible with a three dimensional periodic structure. However, all the peak positions can be written as integer linear combinations of finitely many basic wave vectors. This fact allows to view these structures as intersections of physical space with a higher-dimensional periodic structure.

In chapter one, we introduce a broad class of discrete structures which produce diffraction patterns of the desired type. We discuss various properties of these structures. In particular, we show that they are almost periodic, where we have used a definition of almost periodicity which is an adaption of Bohr's definition suitable for discrete structures. Moreover we elucidate the connection between the intensities of the Fourier spectrum and the concept of local isomorphism.

Next, we start an investigation of the crystallography of quasicrystals. Crystallographic concepts can be applied to quasicrystals because of the connection of quasicrystals to higher-dimensional periodic structures. We show how Bravais classes, point groups and space groups can be defined for quasicrystals, and discuss the experimental consequences of these symmetries. In chapter two, we give a complete list of quasicrystal Bravais classes for those point symmetries which require a higherdimensional structure of dimension at most six. Then, in chapter three, we derive a complete list of point groups and space groups belonging to the five dimensional Bravais classes of chapter two. These are those space groups whose point group is in three dimensions (2+1)-R-reducible. For these space groups, we give the non-primitive translations and the characteristic extinction patterns of the Fourier spectrum.

In chapter four, various construction methods for quasiperiodic tilings are described. After reviewing the classical grid-projection technique, we introduce a generalisation of it, which allows the generation of tilings with arbitrary point symmetry (in Fourier space) with the help of lattices whose dimension is the minimal one required by the point symmetry. Moreover, we discuss a hierarchic construction invented by Stampfli and relate it to other construction methods. Thereby we prove that the tilings produced by Stampfli's algorithm are indeed quasiperiodic.

In chapter five we introduce a detailed model structure for quasicrystals with dodecagonal symmetry. This model structure specifies all atomic positions and is derived from closely related periodic phases which always occur together with dodecagonal quasicrystals. Moreover, this model structure is particularly well suited to illustrate the crystallographic concepts introduced earlier. We derive the point group as well as the space group of this structure. The space group is of special

crystallographic interest, since it is a non-symmorphic one. It contains a screw axis as well as a set of glide mirror planes. We calculate the electron diffraction patterns of the model structure for various directions of the incident beam. This calculation includes multiple scattering effects, which are very important for electron diffraction. The calculated diffraction patterns agree very well with the experimentally observed ones. We verify that the systematic extinctions coincide with those predicted by the previous space group analysis.

Introduction

In 1984, Shechtman et al. [S] reported about a novel phase they had observed in rapidly quenched *Al-Mn* alloys. This phase had two striking properties which at first sight seemed to be incompatible with each other. On the one hand, in electron diffraction experiments this new material produced sharp diffraction peaks, as it is usually observed for crystals. On the other hand however, the positions and intensities of these diffraction peaks displayed icosahedral symmetry, which is not compatible with a three dimensional periodic structure. It is easy to show that three dimensional crystals cannot have icosahedral symmetry. Let A be one of the five-fold rotations contained in the icosahedral group. If A is the symmetry of a 3d crystal lattice L, the matrix of A expressed with respect to a lattice basis has only integer entries. In particular, it has an integer trace. On the other hand, there exists an orthonormal basis with respect to which the matrix of A reads

$$A = \begin{pmatrix} \cos(\frac{2\pi}{5}) & -\sin(\frac{2\pi}{5}) & 0 \\ \sin(\frac{2\pi}{5}) & \cos(\frac{2\pi}{5}) & 0 \\ 0 & 0 & 1 \end{pmatrix}. \tag{0.1}$$

From (0.1) it follows that A has trace $2\cos(\frac{2\pi}{5}) + 1$, which is irrational and not an integer. Hence, five-fold rotations and therefore icosahedral symmetry are not compatible with a 3d lattice. Compatible with a 3d lattice are only rotations of order 2, 3, 4 or 6.

The question therefore arose which structure could produce the strange diffraction patterns observed by Shechtman et al. A first hint was given by an optical diffraction pattern of a Penrose pattern [Pen, Ga] published earlier by Mackay [M1], which was ten-fold symmetric. Penrose patterns are non-periodic tilings of the plane composed of two different tiles, a 36° and a 72° rhombus* [Pen, Ga]. Mackay's work clearly showed that the Penrose patterns could provide a solution to this puzzling problem.

Levine and Steinhardt [LS1] were the first who tried to explain the novel diffraction patterns by means of a three dimensional, icosahedrally symmetric version of the Penrose patterns. They introduced the term "quasicrystal" for structures of this type. Most subsequent authors however preferred a different kind of generalization, based on de Bruijn's [dB1] algebraic theory of Penrose patterns. In his famous papers [dB1], de Bruijn characterized the Penrose patterns as the dual graphs of certain simple grids. More importantly, he also showed that they can be obtained as the projections of certain lattice hypersurfaces in a 5d cubic lattice. de Bruijn's

*we will always refer to these Penrose rhombus patterns, not to their kite and dart versions [Pen, Ga]

ideas were soon taken up by other authors. Kramer and Neri [KN] published a 3d icosahedrally symmetric version of the Penrose pattern, obtained by projection from six dimensions, still before Shechtman's discovery. Their structure is composed of two types of rhombohedra earlier described by Mackay [M2]. After Shechtman's paper was published, Elser [E1] and independently Duneau and Katz [DK] used Kramer and Neri's structure as a model for Shechtman's new phase. They also calculated the Fourier spectrum of this model structure, and it turned out that — in contrast to Levine and Steinhardt's model — they could explain the peak positions and, qualitatively, even the intensities of Shechtman's diffraction patterns. A very similar model had also been proposed by Kalugin et al. [Ka].

de Bruijn's theory soon was generalized to arbitrary point symmetry [SSL, GR]. This was important because meanwhile several other quasicrystal phases had been observed, some in materials having different composition but the same point symmetry, others having different point symmetry, e. g. ten-fold [Be, F], twelve-fold [INF1], and, most recently, eight-fold [WCK]. The term "quasicrystal" was adopted also for these phases and their respective model structures. For the moment, the term "symmetry" applies only to Fourier space — in real space no symmetry is apparent. We will see later in which sense symmetry is present also in real space.

Instead of simply applying de Bruijn's ideas to other symmetries and lattices, we aim at a more general approach to quasicrystals. These novel phases all have the property that their Fourier spectrum consists of sharp Bragg peaks, and that the positions of all these peaks can be written as integer linear combinations of finitely many basic wave vectors, $\mathbf{k}_1, \ldots, \mathbf{k}_n$. Such structures are called *quasiperiodic*; this is another justification of the term quasicrystal. Therefore, a quasicrystal structure can be written as a Fourier series:

$$\rho(\mathbf{x}) = \sum_{\mathbf{m} \in Z^n} a_{\mathbf{m}} e^{i\mathbf{x} \cdot \sum_{i=1}^{n} m_i \cdot \mathbf{k}_i}. \tag{0.2}$$

The only difference to a periodic structure is that we need more basic wave vectors than we have space dimensions. The Fourier series (0.2) suggests, however, that a quasiperiodic structure is related to a periodic structure in a higher-dimensional space. If n basic wave vectors are required, we can embed d-dimensional physical space $E^{\parallel}$ in an n-dimensional space E and add a sub- or superscript $\parallel$ to all quantities existing in physical space. To each basic wave vector $\mathbf{k}_i^{\parallel}$ we then add a component $\mathbf{k}_i^{\perp}$ contained in the orthogonal complement $E^{\perp}$ of $E^{\parallel}$, so that the vectors $\mathbf{k}_i = \mathbf{k}_i^{\parallel} + \mathbf{k}_i^{\perp}$, $i = 1, \ldots, n$, become linearly independent. Our quasiperiodic structure can then be viewed as the restriction of an n-dimensional periodic structure to a d-dimensional subspace:

$$\rho(\mathbf{x}^{\parallel}) = \sum_{\mathbf{m} \in Z^n} a_{\mathbf{m}} e^{i\mathbf{x}^{\parallel} \cdot \sum_{i=1}^{n} m_i \cdot \mathbf{k}_i}. \tag{0.3}$$

Hence, with each quasiperiodic structure a higher-dimensional periodic structure is associated. We therefore study the question whether the symmetries of quasicrystals can be explained in terms of symmetries of the higher-dimensional structure, and which crystallographic concepts developed for periodic structures are applicable also for quasicrystals (through the related higher-dimensional structure) and lead to observable effects. This is essentially the subject of this work.

In the first chapter, we discuss various properties of general discrete quasiperiodic structures. In particular, Bohr's definition (see e. g. [Bes]) of almost-periodicity in terms of real space properties, which applies to uniformly continuous functions, is adapted to discrete structures, and it is proved that the popular models for quasicrystals are almost periodic in this sense (note that almost periodic structures are more general than quasiperiodic ones — their Fourier transform may consist of an arbitrary countable set of Bragg peaks). The Fourier spectrum of such structures is calculated, and its relation to local isomorphism is elucidated.

In chapter two, we start an investigation of the crystallography of quasicrystals. In this chapter, we explain how Bravais classes and point groups can be defined for quasicrystals, and we give a complete list of quasicrystal Bravais classes for the cases which require a higher-dimensional structure with a dimension of maximally six. These Bravais classes are characterized in detail.

In chapter three, we introduce space groups for quasicrystals and explain how they can be observed experimentally by means of their characteristic extinctions. A complete list of those space groups is given which fall into the five dimensional Bravais classes described in chapter two. These are those space groups whose point group is in three dimensions (2+1)-R-reducible. For each of these space groups, the non-primitive translations and the characteristic extinction pattern is given.

In chapter four, we describe various methods to construct quasiperiodic tilings. Besides of a description of de Bruijn's grid-projection technique and of its early generalisations, we introduce a generalisation [KGR] which allows the generation of tilings with arbitrary point symmetry without necessity to use a lattice of dimension higher than the minimal dimension required by the point symmetry. This technique has already implicitly been used by Stampfli [St] for a special case. Moreover, we describe a hierarchic construction also developed by Stampfli [St], and relate it to other construction methods, proving thereby that the tilings produced by it are indeed quasiperiodic.

In chapter five we construct a detailed model structure, including atomic positions, for dodecagonal quasicrystals [INF1, INF2, CLK]. The purpose of this chapter is two-fold. Firstly, such detailed model structures which include atom positions are still rare for quasicrystals. In fact, they exist only for two different icosahedral phases [EH, HE]. In the dodecagonal case, high resolution electron micrographs

and the knowledge of closely related periodic phases allow for the construction of a model structure which seems to be a good candidate of a structure containing the essential features of the true structure. Secondly, this model structure illustrates all the crystallographic concepts developed earlier. It has a crystallographically interesting, non-symmorphic space group which contains a screw axis and a set of mirror glide planes. We demonstrate how these space group elements lead to characteristic extinctions in the Fourier spectrum. Unfortunately, due to experimental difficulties, the peaks predicted to be extinct are at present not accessible by experiment, so that these extinctions could not yet be checked against electron diffraction results.

Chapter One

Discrete Quasiperiodic Structures

1.1 The Projection Method

In the introduction we have seen that quasiperiodic structures can be viewed as the restriction of a higher-dimensional periodic structure to a suitably embedded subspace. We first construct a suitable class of such periodic structures which lead to discrete quasiperiodic structures. Let L be a lattice in E^n, generated by a basis $\mathbf{e}_1, \ldots, \mathbf{e}_n$, $E^\parallel$ a d-dimensional subspace of E^n, and $E^\perp$ its orthogonal complement, so that $E^n = E^\parallel \oplus E^\perp$. Denote by $P^\parallel$ and $P^\perp$ the orthogonal projectors onto $E^\parallel$ and $E^\perp$ respectively, so that any vector $\mathbf{x} \in E^n$ can be decomposed as $\mathbf{x} = \mathbf{x}_\parallel + \mathbf{x}_\perp$, where $\mathbf{x}_\parallel = P^\parallel \mathbf{x}$ and $\mathbf{x}_\perp = P^\perp \mathbf{x}$.

The periodic structures we consider are given by

$$f(\mathbf{x}) = \int d\mathbf{y}\, s(\mathbf{y}) m(\mathbf{x} - \mathbf{y}), \tag{1.1}$$

where

$$s(\mathbf{x}) = \sum_{\mathbf{z} \in L} \delta(\mathbf{x} - \mathbf{z}) \tag{1.2}$$

is the density of the lattice L, and

$$m(\mathbf{x}) = \delta(\mathbf{x}_\parallel) \chi_C(\mathbf{x}_\perp) \tag{1.3}$$

is the density of the motif with which L is decorated. In (1.3) χ_C denotes the characteristic function of an open domain $C \subset E^\perp$ with compact closure. Therefore, each lattice point of L is decorated with a motif which is a piece of a $(n-d)$-dimensional subspace parallel to $E^\perp$ with the shape of C. The quasiperiodic structures to be considered here are given by the restriction of $f(\mathbf{x})$ to a d-dimensional subspace E parallel to $E^\parallel$:

$$\rho_\gamma(\mathbf{x}_\parallel) = f(\mathbf{x}_\parallel + \gamma_\parallel, \gamma_\perp). \tag{1.4}$$

The quasiperiodic structures (1.4) are labelled by the vector γ pointing from the origin of L to the (freely chosen) origin of E.

The same class of structures can be obtained also by an alternative method. We first note that the motif m (1.3) attached at a lattice point $\mathbf{x}$ intersects E if and only if $\gamma_\perp \in \mathbf{x}_\perp + C$, or, alternatively, $\mathbf{x}_\perp \in \gamma_\perp - C$. Therefore, the structure

ρ_γ can be obtained by projecting all those lattice points $\mathbf{x}$ of L onto E for which $\mathbf{x}_\perp \in \gamma_\perp - C$ holds:

$$\rho_\gamma(\mathbf{x}_\parallel) = \sum_{\mathbf{z}\in(L\cap S)} \delta(\mathbf{x}_\parallel + \gamma_\parallel - \mathbf{z}_\parallel), \tag{1.5}$$

where the strip S is given by

$$S = \{\mathbf{x} | \mathbf{x}_\perp \in \gamma_\perp - C\}. \tag{1.6}$$

This latter formulation is known as the projection method [DK, E1].

1.2 Finite Subpatterns and Local Isomorphism

In this section we discuss some properties of the distributions $\rho_\gamma(\mathbf{x}_\parallel)$, or, alternatively, of the set of quasilattice points,

$$Q_\gamma = \{\mathbf{x}_\parallel \in E | \rho_\gamma(\mathbf{x}_\parallel) \neq 0\} = \{\mathbf{x}_\parallel - \gamma_\parallel \in E | \mathbf{x} \in S \cap L\}. \tag{1.7}$$

If $E^\parallel$ contains any lattice vectors of L, and thus a whole sublattice of L, then these lattice vectors are translation symmetries of our patterns. Since we are interested mainly in nonperiodic patterns, we assume in the following that there are no lattice vectors of L contained in $E^\parallel$.

Let us consider the dependence of Q_γ on γ. From (1.7) it becomes clear that a change of $\gamma_\parallel$ amounts just to a translation of the pattern. Similarly, changing γ by a lattice vextor $\mathbf{x}$ yields again the original pattern, translated by $\mathbf{x}_\parallel$. These are the only symmetries of this kind however: more general changes of γ yield patterns which are truely different. Therefore, two patterns with parameters γ and γ' are translation equivalent iff

$$\Delta\gamma_\perp = \gamma_\perp - \gamma'_\perp \in P^\perp L. \tag{1.8}$$

Let K be the closure of $P^\perp L$. This set has the structure

$$K = \Lambda^m \times E^{m'}, \quad m + m' = n - d, \tag{1.9}$$

where Λ^m is an m-dimensional lattice. Note that Λ^m needs not be generated by lattice vectors.

Consider now a finite subpattern $F^\parallel \subset Q_\gamma$, and let $\mathbf{x}_\parallel$ be one of its vertices. We call $\mathbf{x}_\parallel$ the origin of $F^\parallel$. There is a unique set F of lattice points in the strip S which projects onto the vertices of $F^\parallel$. Since the cross section of S is open, the set F can be moved in a finite domain $U \subset E^\perp$ without leaving the strip. This implies that vertices $\mathbf{x}$ which project into U are the origin of a translation of F which is also contained in S. There are infinitely many such lattice points, and so each finite subpattern of Q_γ occurs infinitely often in Q_γ. Since L projects with a

uniform density onto K [KNi], the relative number of vertices which are the origin of a subpattern F is equal to the ratio $\mu(K \cap U)/\mu(K \cap (\gamma_\perp - C))$, where μ is the m'-dimensional Lebesque measure.

Next we compare two patterns Q_γ and $Q_{\gamma'}$. If $\gamma_\perp - \gamma'_\perp = \Delta\gamma_\perp \in K$, then there exists a sequence of patterns Q_{γ^n} such that Q_{γ^n} is a translation of Q_γ and $\gamma^n_\perp$ converges to $\gamma_\perp$. On the other hand, such a sequence exists only if $\Delta\gamma_\perp \in K$. Now observe that two patterns with parameters γ and γ' agree in regions of radius R centered at $\gamma_\parallel$ and $\gamma'_\parallel$ respectively if only $|\Delta\gamma_\perp|$ is small enough. This follows from an analysis similar to that in the preceeding paragraph. Instead of moving the set F without leaving the strip, we can hold F fixed and move the strip. Therefore we have proved that every finite portion of a pattern Q_γ occurs also in $Q_{\gamma'}$ if and only if $\Delta\gamma_\perp \in K$. If this is the case, this finite subpattern occurs even infinitely often, and with the same density in both patterns.

Two quasiperiodic patterns which have the property that each finite portion of one occurs also in the other, and vice versa, are called *locally isomorphic*. Therefore, we have proved that two patterns Q_γ and $Q_{\gamma'}$ are locally isomorphic if and only if $\Delta\gamma_\perp \in K$. Local isomorphism is a concept which has been introduced in the context of quasicrystals by Levine and Steinhardt [LS2].

1.3 Estimate on the Number of Finite Subpatterns

Next, we estimate the number $N(R)$ of different neighbourhoods of radius R a vertex of a quasicrystal pattern Q_γ (1.7) can have. This is done as follows. Choose a lattice site $\mathbf{x} \in L$ and a ball $B(R) \subset E^\parallel$ of radius R, centered at $\mathbf{x}_\parallel$, and move the strip S through $E^\perp$, but subject to the conditions that i) $\mathbf{x} \in S$ and ii) the local isomorphism class is preserved, and count the number of patterns distinct in $B(R)$ we pick up in this way. The lattice sites $\mathbf{y} \in L$ which are projected onto a vertex of at least one of these patterns have the property that i) $\mathbf{y}_\parallel \in B(R)$ and ii) $\mathbf{y}_\perp \in C' \subset E^\perp$, where C' is a compact domain which is independent of R (roughly speaking, the diameter of C' is twice that of the set C). Therefore the number of these vertices, $n(R)$, can be bounded by $n(R) \leq \text{const.} \cdot V(R)$, where $V(R)$ is the volume of $B(R)$.

The translations of the strip which preserve the local isomorphism class consist of m' independent continuous translations and a lattice Λ^m of discrete translations (compare section 1.2). The condition that $\mathbf{x} \in S$ restricts this to continuous translations in a compact domain and finitely many discrete translations.

Under a continuous translation new vertices enter the strip, others leave the strip. However, they enter and leave the strip in a fixed order and therefore under a continuous translation we pick up at most $2n(R)$ patterns. Since there are m'

independent continuous translations we obtain a bound

$$N(R) \leq \text{const.} \cdot V(R)^{m'}. \tag{1.10}$$

Note that the finite number of discrete translations can affect only the constant in (1.10).

The bound (1.10) can be applied to the termodynamics of quasicrystals. Suppose that a quasicrystal pattern describes the ground state of a physical system with finite range interactions. Since in two locally isomorphic patterns every finite portion occurs with the same density, a finite range interaction cannot distinguish the two patterns. Therefore we conclude that all locally isomorphic patterns (uncoutably many!) describe energetically degenerate states. Nevertheless, there is no residual (zero temperature) entropy density to be expected. Since the number $N(R)$ of different configurations in a volume $V(R)$ grows at most with a power of R, in the termodynamic limit we have

$$s(T=0) = k \cdot \lim_{R\to\infty} \frac{1}{V(R)} \ln N(R) = 0. \tag{1.11}$$

This result can be understood intuitively also from the fact that the whole quasicrystal pattern is completely specified by finitely many real parameters (the components of the vector γ).

1.4 Quasiperiodicity

Let us now consider two patterns Q_γ and $Q_{\gamma'}$ which are translates of each other, i. e. $\Delta\gamma \in P^\perp L$. What is the fraction of the vertices of one pattern occuring also in the other? These vertices are projections of lattice points which occur in the strips of both patterns, i. e. they satisfy

$$\mathbf{x}_\perp \in (\gamma_\perp - C) \cap (\gamma'_\perp - C). \tag{1.12}$$

Clearly, the fraction of these vertices is

$$q = \frac{\mu((\gamma_\perp - C) \cap (\gamma'_\perp - C) \cap K)}{\mu((\gamma_\perp - C) \cap K)}, \tag{1.13}$$

where μ is again the m'-dimensional Lebesque measure. If we keep $\Delta\gamma_\perp$ small, then q is close to 1. More precisely, for each positive ratio $q < 1$ we can find a neighborhood $U \subset E^\perp$ of the origin such that all lattice vectors $\mathbf{x}$ which project into U have the property that a pattern and its translation by $\mathbf{x}_\parallel$ agree on at least a fraction q of their vertices. Let us now study this set of almost translation symmetries in more detail.

DEFINITION: A set $X \subset E^n$ is called *relatively dense* if there exists $R < \infty$ such that any ball $B(R) \subset E^n$ of radius R contains at least one point of X.

THEOREM. *Let $q < 1$, and let X be the set of vectors $\mathbf{x}_\parallel \in E^\parallel$ such that the translation of a pattern Q_γ by $\mathbf{x}_\parallel$ agrees on a fraction q of the vertices with the original pattern. Then X is relatively dense in $E^\parallel$.*

PROOF: It is sufficient to prove that any quasicrystal pattern of the type (1.7), no matter how small the (open) cross section of the strip S is (as long as it cuts the set K (1.9)), is a relatively dense set. We give here the proof only for a subclass of patterns, to which however all the tilings with crystallographically forbidden point symmetry belong. We cover therefore the physically interesting cases. The proof for the general case is rather complicated. We restrict ourselves to those cases which contain a subpattern which is the product of d 1-dimensional quasicrystals obtained from 2-dimensional sublattices. The directions of these quasicrystals are assumed to be independent. Such a product of 1d quasicrystals exists if there are d different 2d sublattices contained in planes each of which is spanned by a vector $\mathbf{v}_i^\parallel$ in $E^\parallel$ (the direction of the 1d quasicrystal) and a vector $\mathbf{v}_i^\perp$ in $E^\perp$. As acceptance region of the subpattern we choose a parallelohedron (the higherdimensional generalisation of a parallelogram or parallelepiped) which is spanned by vectors $c_i\mathbf{v}_i^\perp$. By choosing the numbers c_i small enough we can always construct an acceptance region for the subpattern which fits into the original acceptance region. We therefore can construct a subpattern which is a product of 1d quasicrystals obtained from 2d lattices. The latter is known to be relatively dense. In fact, in a 1d quasicrystal obtained from a 2d lattice there occur only two, in sigular cases three different intervals [KNi]. ■

This theorem makes the connection to the theory of almost periodic functions of Bohr (see e.g. [Bes]). According to Bohr, a function $f(\mathbf{x})$ is *uniformly almost periodic* iff for each $\epsilon > 0$ there exists a relatively dense set of vectors $\mathbf{x}_i$ such that

$$|f(\mathbf{x}) - f(\mathbf{x} - \mathbf{x}_i)| < \epsilon$$

for all i, uniformly in $\mathbf{x}$. Bohr's almost periodic functions are uniformly continuous, and the translates $f(\mathbf{x}-\mathbf{x}_i)$ are close to $f(\mathbf{x})$ in the uniform topology. This topology is of course not suitable for discrete structures. The natural topology for discrete structures is the one we have used above, in which two structures are close to each other if they disagree only on a small fraction of the vertices. Therefore, if in Bohr's definition we replace the uniform topology by the natural topology for discrete structures, our patterns are almost periodic. Quasiperiodic structures are a special class of almost periodic structures. They satisfy the additional requirement that their frequency module is finitely generated. This is indeed the case for our structures, see next section.

1.5 The Fourier Transform

In this section we compute the Fourier transform of the distributions $\rho_\gamma(\mathbf{x}_\parallel)$ (1.4). Formally, from (1.4) we get

$$\hat{\rho}_\gamma(\mathbf{k}_\parallel) = e^{-i\gamma_\parallel \cdot \mathbf{k}_\parallel} \int d\mathbf{k}_\perp e^{-i\gamma_\perp \cdot \mathbf{k}_\perp} \hat{f}(\mathbf{k}_\parallel, \mathbf{k}_\perp). \tag{1.14}$$

Since $f(\mathbf{x})$ is simply the convolution of $s(\mathbf{x})$ and $m(\mathbf{x})$, its Fourier transform is given by

$$\hat{f}(\mathbf{k}) = \hat{s}(\mathbf{k}) \cdot \hat{m}(\mathbf{k}) = \hat{s}(\mathbf{k}) \cdot \hat{\chi}_C(\mathbf{k}_\parallel). \tag{1.15}$$

Therefore, the Fourier spectrum of ρ_γ is essentially the projection of the Fourier spectrum of f onto $\hat{E}^\parallel$. Each peak gets an additional phase, which is not observable however.

There is a problem arising however. Since χ_C is a discontinuous function, its Fourier transform decays only slowly, and so the amplitudes of the peaks of $\hat{\rho}_\gamma$ contained even in a finite region are not summable. Therefore we have to find a regularisation procedure to give (1.14) a mathematical meaning. One possibility is the use of tempered distributions. Certainly, ρ_γ is a tempered distribution, and so its Fourier transform is defined unambiguously. To get a more explicit result, we construct a sequence of distributions ρ_γ^n which converges to ρ_γ, and for which the formal calculation (1.14) makes sense. The Fourier transform of ρ_γ is then given by $\lim \hat{\rho}_\gamma^n$ (again in the sense of distributions). The distributions ρ_γ^n are obtained by replacing χ_C in (1.3) by smooth approximations χ_C^n which have the properties that i) $0 \leq \chi_C^n \leq 1$ and ii) χ_C^n deviates from χ_C only at points whose distance to the boundary of C is less than $\frac{1}{n}$. Such a sequence clearly converges to χ_C, and since χ_C^n is smooth, its Fourier transform is rapidly decreasing, and so the formal calculation (1.14) makes sense. In the following, all calculations are understood in the sense described above.

If there are no reciprocal lattice vectors contained entirely in $\hat{E}^\perp$, the integration path for fixed $\mathbf{k}_\parallel$ in (1.14) hits at most one peak, i. e. at most one peak is projected onto a given point in $\hat{E}^\parallel$. If we change the vector γ, the phase of each peak is changed, but its intensity remains invariant. If there are reciprocal lattice vectors contained in $\hat{E}^\parallel$ however, the situation is different. Then an infinite array of peaks is projected onto the same spot. Under a change of γ, not necessarily all peaks in this array pick up the same phase, and so interferences might occur which change the intensities. More precisely, whenever $\Delta\gamma_\perp$ has a nonvanishing component in the direction of a lattice vector in $\hat{E}^\parallel$, the intensities will change, whereas if this is not the case they remain invariant. The following theorem relates this to the concept of local isomorphism introduced in section 1.2 (see also [LS2]).

THEOREM. *The Fourier transforms of two quasicrystal patterns agree in intensity if and only if they are locally isomorphic.*

PROOF: Since the local isomorphism class is changed when $\Delta\gamma_\perp$ has a non-vanishing component in the R-span of the lattice vectors spanning the lattice Λ^m (1.9), whereas the intensities of the Fourier transform change if $\Delta\gamma_\perp$ has a non-zero component in the R-span of the reciprocal lattice vectors contained in $E^\perp$, we have to show that these two spaces are the same. Suppose $\mathbf{u}$ is a reciprocal lattice vector contained in $E^\perp$, so that $\mathbf{u} = \sum m_i \hat{\mathbf{e}}_i = \sum m_i \hat{\mathbf{e}}_i^\perp$, or, equivalently, $\sum m_i \hat{\mathbf{e}}_i^\parallel = 0$. Then we have

$$2\pi m_i = \mathbf{e}_i \cdot \sum m_j \hat{\mathbf{e}}_j = \mathbf{e}_i \cdot \sum m_j \hat{\mathbf{e}}_j^\perp$$

and therefore $\mathbf{u} \in \Lambda^m$, since the $\mathbf{e}_i^\perp$ are rationally dependent in the direction of $\mathbf{u}$. Conversely, Λ^m is spanned by vectors $\mathbf{v}_\perp \in E^\perp$ which satisfy $\mathbf{v}_\perp \cdot \mathbf{e}_i = 2\pi m_i$, $m_i \in Z$. But the same holds true also for the lattice vector $\mathbf{w} = \sum m_j \hat{\mathbf{e}}_j$, and since $\{\mathbf{e}_i\}$ is a basis $\mathbf{w}$ must coincide with $\mathbf{v}_\perp$, and therefore $\mathbf{w} \in \hat{E}^\perp$. ■

This result can be understood also in a different way. If there are reciprocal lattice vectors contained in $\hat{E}^\perp$, the set $(\gamma_\perp - C) \cap K$ in general decays into several (but finitely many) connected components. With each of these components C_i, a sublattice L_i of L is associated (the sublattice containing those lattice vectors which project onto C_i). Therefore, the pattern Q_γ can be obtained as a superposition of finitely many subpatterns, constructed from sublattices L_i, and strips with cross section C_i. If we change γ such that $\Delta\gamma_\perp$ has a non-zero component in the direction of a reciprocal lattice vector contained in $\hat{E}^\perp$, the shapes and sizes of the C_i change in general, and it is therefore not surprising that the intensities of the Fourier transform change.

Any quasicrystal structure Q_γ obtained from a lattice whose dimension is larger than the maximal number of rationally independent vectors $\hat{\mathbf{e}}_i^\parallel$ needed to index its Fourier transform can be obtained also from a lattice of lower dimension, but with a more complicated decoration [J1]. In the previous paragraph we have seen that such a pattern can be viewed as the superposition of several quasiperiodic structures Q_i obtained with acceptance regions C_i from lattices L_i. In fact, all these lattices L_i are identical to the same lattice L', but shifted with respect to each other. If the dimension of L' is n', a n'-dimensional periodic structure $f(\mathbf{x})$ such that its restriction to E yields Q_γ is now easily constructed: $f(\mathbf{x})$ is simply the superposition of the corresponding n'-dimensional periodic structures $f_i(\mathbf{x})$ the restriction to E of which yield the patterns Q_i. The periodic density $f(\mathbf{x})$ is based on the lattice L', and each unit cell contains severeral "atoms" a_i, each one with its own acceptance region C_i. If we change the vector γ such that $\Delta\gamma$ has a non-zero component in the direction of a reciprocal lattice vector contained in $\hat{E}^\perp$, the decoration of the unit cell of L' is changed, and therefore also its Fourier transform.

In order to avoid changes in the local isomorphism class under a change of γ, we will work in the following mainly with lattices of minimal dimension. This is no restriction on the class of structures which can be obtained.

Chapter Two
Bravais Classes for Quasicrystals

2.1 Introduction

As we have seen earlier, the Fourier spectrum of a quasicrystal consists of sharp Bragg peaks which can be indexed with finitely many basic wave vectors $\mathbf{k}_1, \ldots, \mathbf{k}_n$. The set $\mathcal{M}$ of all integer linear combinations of peak positions, i. e. the Z-span of $\mathbf{k}_1, \ldots, \mathbf{k}_n$, is a is a finitely generated, free Z-module. $\mathcal{M}$ is called the frequency module of the quasicrystal. We assume that $\mathbf{k}_1, \ldots, \mathbf{k}_n$ is a basis of $\mathcal{M}$, i. e. there is no subset of $\mathbf{k}_1, \ldots, \mathbf{k}_n$ which generates $\mathcal{M}$. Every basis of a finitely generated, free Z-module has the same cardinality, which is called its rank or dimension. For quasicrystals, the rank of the frequency module exeeds the space dimension. Moreover, it is invariant under a point group $G \subset O(3)$ which is not compatible with a 3-dimensional lattice of translation symmetries.

The existence of a finitely generated frequency module implies that the quasicrystal structure can be obtained as the restriction of an n-dimensional periodic structure $f(\mathbf{x})$ to a suitably embedded 3-space E which will be identified with physical space. $\mathcal{M}$ is then the projection of the reciprocal lattice of this periodic structure onto $\hat{E}$.

Given this connection, Bravais classes for quasicrystals can be introduced in two different, but equivalent ways. On the one hand, we can work completely in 3-dimensional space and classify the set of different frequency modules compatible with a given point group G. Two frequency modules are considered as different if they cannot be brought into coincidence by a linear transformation which commutes with G. To restrict the number of possible cases we confine ourselves to modules of minimal rank (number of generators required) compatible with the symmetry G. This approach has been chosen in [RMW].

On the other hand, we can use the Bravais classification of n-dimensional lattices. In the context of quasicrystals, we are interested only in Bravais classes whose point group $\tilde{G} \subset O(n)$ is isomorphic to a 3-dimensional point group $G \subset O(3)$. The action of $\tilde{G}$ is supposed to be reducible, leaving invariant a 3-dimensional subspace $\hat{E}$, and the action of $\tilde{G}$ on $\hat{E}$ is identical to that of G. Such Bravais classes will be called quasicrystal Bravais classes. Clearly, the frequency module $\mathcal{M}$ of a quasicrystal associated with a Bravais lattice L has to be identified with the projection of the reciprocal lattice $\hat{L}$ onto $\hat{E}$. Again, we work only with minimal dimensions, i. e. the dimension of L is equal to the minimal rank of a frequency module compatible with the symmetry G. The advantage of this latter approach is that one obtains

a classification in terms of equivalence classes of n-dimensional periodic structures, to which conventional crystallography can be applied. In particular, the concept of space group can be introduced for a quasicrystal. Non-symmorphic space group symmetries may be experimentally observable in terms of characteristic extinctions (see next chapter). Therefore, we will adopt this latter approach.

A connection between the two approches can be obtained in the following way. If we express the elements of the point group of $\mathcal{M}$ with respect to a Z-basis of $\mathcal{M}$, we obtain a finite unimodular group $B \subset GL_n(Z)$, which is in fact a Bravais group in n dimensions, determining a unique (quasicrystal) Bravais class of lattices. This Bravais group, which is the full point group of the associated Bravais lattice expressed in terms of a lattice basis, determines the representation with which $\tilde{G}$ acts on $\hat{L}$. In particular, the groups B and $\tilde{G}$ are isomorphic, $\tilde{G} = ABA^{-1}$, with an isomorphism $A \in GL_n(R)$. From the action of B the reciprocal lattice $\hat{L}$ can be explicitly constructed. Clearly the 3-dimensional representation G occurs in B and thus in $\tilde{G}$.

Which are the interesting point groups? There are only very few truly 3-dimensional (irreducible) finite subgroups of $O(3)$, namely the invariance groups of the platonic solids and some of their subgroups. Among these only the icosahedral group – with or without inversion – is crystallographically forbidden. All the other finite subgroups of $O(3)$ are (2+1)-R-reducible. Among these the crystallographically forbidden ones are those which have elements of order 5, 7 or more. These elements are either a rotation axis or a rotation followed by an inversion. If inversion is a symmetry by itself, as is the case for the point group of a frequency module, even a true rotation axis of that order is present. We will restrict ourselves to the cases where elements or order 5, 8, 10 or 12 are present. On the one hand these are the ones which have been experimentally observed [Be, F, WCK, INF1] (except for fivefold symmetry, which is closely related to tenfold symmetry however). On the other hand, these groups require only lattices or frequency modules of dimension (rank) five, whereas for all other choices one would need at least dimension seven.

For all these symmetries it is easy to determine the decomposition of $\tilde{G}$ into R-irreducible components. The key observation is that any linear mapping leaving a lattice invariant has integer trace, for if we express it in terms of a lattice basis its matrix has only integer entries. Since the trace does not depend on the basis which is used, the representation matrices of any representation $\tilde{G}$ which leaves a lattice invariant must have integer traces, i. e. the character of this representation must be integer for all conjugation classes. The 3-dimensional representation G doesn't fulfill this requirement, but occurs in $\tilde{G}$. Terefore, we have to add more irreducible representations in such a way that the total character becomes integer on all conjugation classes. It turns out that for the groups under consideration

there exists a unique choice such that the total dimension is equal to the rank of the frequency module. The representation constructed in this way must therefore coincide with $\tilde{G}$.

2.2 Lattices with (2+1)-Reducible Point Groups

In this section we consider frequency modules whose point group G leaves a 1-dimensional space (the z-axis, say) and its orthogonal complement separately invariant. It is assumed that G contains rotations by an angle of $\frac{2\pi}{p}$ ($p = 5$, 8, 10 or 12) around the z-axis. Since G is (2+1)-reducible, the action of any element of G on the z-axis is plus or minus the identity. Therefore, frequency modules of minimal dimension and compatible with G have the property that the z-components of all their elements are contained in $c\mathrm{Z}$, c a fixed number.

Let us first consider the z=0 plane of $\mathcal{M}$, which is a submodule $\mathcal{M}' \subset \mathcal{M}$. Also $\mathcal{M}'$ is of course a finitely generated free Z-module. Let us choose one vector a of a basis of $\mathcal{M}'$ and act repeatedly with the p-fold rotation A on it. The Z-span of the p vectors obtained in this way is a frequency module $\mathcal{M}''$, the simplest frequency module invariant under p-fold rotation symmetry. For the p's under consideration it is easy to see that $\mathcal{M}''$ has rank four. For each natural number q, $1 < q < p$, which is not coprime with p, A^q generates a proper subgroup of C_p. The vectors in an orbit of this subgroup add up to zero, i. e. there is a linear relation between these vectors. The subgroup generated by A^q has q such orbits. To count the number of independent linear relations we proceed as follows. For each such independent relation we remove a number from the set $S = \{1, \ldots, p\}$. The cardinality of the resulting set then is the rank of the module. Since any frequency module is inversion symmetric, there is always a subgroup of C_p of order two (p=5 does not occur for the submodule in the z=0-plane), which has $\frac{p}{2}$ different orbits leading to $\frac{p}{2}$ independent relations. For these $\frac{p}{2}$ relations we remove the even numbers, i. e. those which are divisible by the order of the subgroup. Then we proceed with the subgroup of the next higher order q coprime with the previously considered orders, this time coprime with 2. A subgroup with an order not coprime with the previously considered orders would not give new independent relations, for its orbits are unions of entire orbits of subgroups of smaller order. The subgroup of order q has $\frac{p}{q}$ orbits. However, half of the corresponding relations are independent, for the C_2-subgroup of C_p maps C_q-orbits onto each other and thus these relations are equivalent. To account for these relations, we remove from S the numbers divisible by q. Note that half of them have been removed already in the first step, so that we are counting correctly. Then we proceed in the same way with the subgroup of the next higher order which is coprime with the previously considered orders, and so on. Each time we remove from S those numbers which are divisible by the order of the present subgroup. The

number of eliminated elements of S is alway equal to the number of newly generated inequivalent relations. In the end S contains only the numbers which are relatively prime with p. There are $\phi(p)$ such numbers, where $\phi(p)$ is Eulers function. For $p = 8, 10$ and 12, $\phi(p)$ is equal to four, whereas for other $p > 6$ we obtain for $\phi(p)$ at least 6. This is one of the reasons to restrict ourselves to the cases $p = 5$, 8, 10 and 12.

$\mathcal{M}''$ is certainly a submodule of $\mathcal{M}'$. If $\mathcal{M}' = \mathcal{M}''$ we have characterized the $z = 0$ plane of $\mathcal{M}$. If $\mathcal{M}''$ is a proper submodule of $\mathcal{M}'$ we note that since we consider only modules of minimal rank the two ranks must be equal. Therefore the factor module $\mathcal{M}^f = \mathcal{M}'/\mathcal{M}''$ must be finite (it is a pure torsion module). $\mathcal{M}'$ is a finite union of equivalence classes,

$$\mathcal{M}' = \bigcup_{a \in \mathcal{M}^f} (a + \mathcal{M}''). \tag{2.1}$$

In other words, $\mathcal{M}'$ is a centering of $\mathcal{M}''$. This can be seen also in a different way. Since $\mathcal{M}^f$ is a torsion module, for each element $a \in \mathcal{M}^f$ there exists an integer n such that $na = 0 \pmod{\mathcal{M}''}$. Let m be the least common multiple of these integers. Then $\mathcal{M}''$ is a submodule of $\frac{1}{m}\mathcal{M}'$.

It has been shown [MRW] that for even p's up to $p = 44$ there are no centerings of $\mathcal{M}''$. For the p's under consideration, this can be seen also from a comparison with the classification of Bravais groups in four dimensions. Since all the modules $\mathcal{M}'$ (for fixed p) have the same point group $G \subset O(2)$ it is sufficient to construct the representation $\tilde{G}$ and to verify that there is just one Bravais lattice with symmetry $\tilde{G}$.

The generator A of C_p acts with the representation

$$A^{\parallel} = \begin{pmatrix} \cos(\frac{2\pi}{p}) & -\sin(\frac{2\pi}{p}) \\ \sin(\frac{2\pi}{p}) & \cos(\frac{2\pi}{p}) \end{pmatrix} \tag{2.2}$$

on $\mathcal{M}''$. This representation we have to supplement with another 2-dimensional representation of C_p such that the total character becomes an integer. For all the p's we are interested in there is a unique choice (up to equivalence), namely

$$A^{\perp} = \begin{pmatrix} \cos(q\frac{2\pi}{p}) & -\sin(q\frac{2\pi}{p}) \\ \sin(q\frac{2\pi}{p}) & \cos(q\frac{2\pi}{p}) \end{pmatrix} \tag{2.3}$$

where $q(p)$ is the (unique) natural number $< \frac{p}{2}$ which is coprime with p and different from 1 (note that q and $p - q$ determine equivalent representations so that we can restrict q to be less than $\frac{p}{2}$). Clearly, we have $q(5) = 2$, $q(8) = q(10) = 3$ and $q(12) = 5$.

A (reciprocal) lattice projecting onto $\mathcal{M}''$ is now easily constructed. The lattice vector projecting onto the first basis vector of $\mathcal{M}''$ must have components in both the representation spaces of $A^{\parallel}$ and $A^{\perp}$. These components we can choose arbitrarily – invariant under orthogonal changes of coordinates are only the lengths of the projections on these spaces, $a_{\parallel}$ and $a_{\perp}$. By acting with $A = A^{\parallel} \oplus A^{\perp}$ on this vector and then taking the Z-span we obtain a 2-parameter family of lattices. The lattice parameter $a_{\parallel}$ is determined by the scale of $\mathcal{M}''$, whereas the parameter $a_{\perp}$ has no physical significance. Comparison with [Br] shows that these lattices belong to the octagonal, decagonal and dodecagonal Bravais class in four dimensions (p=5 and p=10 both lead to decagonal lattices). These Bravais classes are known to have no centerings [Br].

For special choices of the ratio of the parameters $a_{\parallel}$ and $a_{\perp}$, we obtain lattices in a different Bravais class, with a larger point symmetry. In particular, in the octagonal case we obtain for $a_{\parallel} = a_{\perp}$ hypercubic primitive and for $a_{\parallel} = (1+\sqrt{2})a_{\perp}$ hypercubic Z-centered lattices. In the decagonal case, for $a_{\parallel} = a_{\perp}$ we get icosahedral SN-centered and for $a_{\parallel} = \tau a_{\perp}$ icosahedral primitivee lattices (τ is the golden mean $(1+\sqrt{5})/2$). Finally, in the dodecagonal case for $a_{\parallel} = a_{\perp}$ and $a_{\parallel} = \sqrt{2+\sqrt{3}}a_{\perp}$ we obtain lattices in the diisohexagonal orthogonal primitive and hypercubic Z-centered Bravais classes respectively. All these names refer to the terminology of [Br]. Two remarks are in order. The icosahedral lattices to which decagonal lattices degenerate are invariant under the 4-dimensional irreducible representation of the icosahedral group and therefore cannot be used for the description of 3-dimensional icosahedrally symmetric quasicrystals. Secondly, both octagonal and dodecagonal lattices can degenerate to a hypercubic Z-centered lattice. The point group of the latter therefore contains both 8-fold and 12-fold rotations, which however leave different subspaces invariant.

The Bravais groups of all these lattices are maximally symmetric [Ras]. They contain elements which mix the spaces $E^{\parallel}$ and $E^{\perp}$ left invariant by $A = A^{\parallel} \oplus A^{\perp}$. These symmetry elements can hardly be used for physics, and so from the physical point of view these maximally symmetric Bravais classes can not be distinguished from the less symmetric ones. Nevertheless for the construction of a quasicrystal model structure it may be convenient to use a maximally symmetric lattice (see chapter 4).

Now as we have discussed the z=0 plane of $\mathcal{M}$ in detail we include again the third dimension into our considerations. Let x be the shortest vector in $\mathcal{M}$ which is parallel to the z-axis. This vector has length mc, m an integer. c is the smallest positive z-component a vector in $\mathcal{M}$ may have. The direct sum $\mathcal{M}_0 = \mathcal{M}' \oplus mc\mathrm{Z}$ is a submodule of $\mathcal{M}$ of full rank five. Again we can define the finite factor module $\mathcal{M}/\mathcal{M}_0$ which in this case is either zero (if $\mathcal{M} = \mathcal{M}_0$) or generated by one element

a of order m (i. e. $\mathcal{M}/\mathcal{M}_0$ has m elements). Without restriction we can assume that the z-component of a is c. Now we act with the p-fold rotation A on a and note that if we add the vectors in an orbit of C_p or of any of its subgroups we obtain a vector which is parallel to the z-axis, i. e. contained in $\mathcal{M}_0$. Therefore, if C_p has cyclic subgroups of orders $p_1, \ldots, p_k$, then we have, if $m \neq 1$, $m\mathrm{Z} = p_1\mathrm{Z} + \cdots + p_k\mathrm{Z}$, or in other words, m is equal to the highest common divisor of $p_1, \ldots, p_k$.

Let us apply this to the cases at hand. Since C_5 contains no proper subgroups, in the pentagonal case there indeed exists a centering. This centered module consists of an alternating stacking of five different planes. It is generated by a set of five vectors which all have z-component c and whose projections onto the xy-plane form a 5-fold symmetric star. Since the primitive module $\mathcal{M}_0$ is even 10-fold symmetric, there is a unique fivefold symmetric frequency module or Bravais class, which unambiguously may be called the pentagonal one.

In the decagonal case there is only the primitive module. C_{10} contains subgroups of orders 2 and 5, which have no (nontrivial) common divisor. However, the pentagonal module can be described as a submodule of the decagonal module $\mathcal{M}_{10}$ as follows. Let us choose for a basis of $\mathcal{M}_{10}$ four vectors in a 5-fold symmetric star generating $\mathcal{M}'$ plus a vector of length c parallel to the z-axis (the latter one will be the fifth basis vector). Then the pentagonal module consists of those vectors of $\mathcal{M}_{10}$ whose indices satisfy $\sum_{i=1}^{4} n_i = n_5 \bmod 5$.

The group C_8 contains subgroups of orders 2, 4 and 8. These orders are not coprime, and therefore there exists a centering also in this case. Here, we have only two different layers. They are best described by viewing this module as a centering of the primitive octagonal module. If one uses a basis analogous to that in the primitive decagonal module, the condition is $\sum_{i=1}^{4} n_i = n_5 \bmod 2$ or $\sum_{i=1}^{5} n_i = \textit{even}$. Therefore, in the octagonal case there are two Bravais classes.

In the decagonal case there is just the primitive module. C_{12} has (among others) subgroups of orders 2 and 3, which are relatively prime.

Clearly, these modules can be lifted to five dimensional lattices in the same way as we have lifted the $z = 0$ planes to four dimensional lattices. These 5d lattices are just stackings of the four dimensional lattices resulting from the layers $z = \text{const}$. Five dimensional lattices have been completely classified by Plesken [P]. In Plesken's classification, the two octagonal modules belong to the two Bravais classes in the crystal family XXIII. The primitive module corresponds to Bravais group B.XXIII.1.1, the centered one to B.XXIII.1.2. The dodecagonal module corresponds to the single Bravais class in crystal family XXIV. The decagonal module corresponds to Bravais group B.XXV.1.1, the pentagonal to B.XXV.1.2, both in crystal family XXV. Therefore, in conclusion, we find a total of five Bravais classes for the p's under consideration. Generators of the point groups of these lattices in

terms of a lattice basis can be found in [P] or in chapter 3.

All the lattices discussed above have 3 parameters, two of which are physically relevant. Again, for special choices of the parameters we obtain lattices of even higher (but non-physical) symmetry. We will not discuss this here in detail, but only mention that for an appropriate choice of the parameters the pentagonal Bravais lattice degenerates to a 5-dimensional hypercubic one. This lattice is relevant for the construction of the famous 2-d Penrose pattern.

2.3 Icosahedral Lattices

In this section we discuss frequency modules invariant under the icosahedral group I, as well as the lattices associated with them. In the last section, we have constructed the simplest C_p invariant modules by acting with C_p on one vector and then taking the Z-span of the set so obtained. In the case of C_p as the essential symmetry of the module, the result was independent of the choice of the starting vector (up to a change of scale and a rotation). In the icosahedral case, this is not true any more. Depending on the stability subgroup of the starting vector, we obtain orbits of different sizes. The smallest orbit is obtained if we choose the starting vector invariant under a C_5 subgroup of the icosahedral group. This orbit consists of twelve vectors pointing to the vertices of an icosahedron, but only six of them are rationally independent (one has to choose one out of each pair of opposite vectors). The module generated by this set will be called the primitive icosahedral module $\mathcal{M}_p$.

It is easy to see that every icosahedrally symmetric module $\mathcal{M}$ must contain a submodule $\mathcal{M}_p$. If we act on any vector $\mathbf{x} \in \mathcal{M}$ repeatedly with a fivefold rotation in I and add the vectors so obtained we get a vector invariant under this fivefold rotation. Acting with I on this vector and taking the Z-span yields a submodule of the type of $\mathcal{M}_p$. This implies that every icosahedrally symmetric frequency module has rank at least six. In the following $\mathcal{M}_p$ denotes the maximal primitive submodule of $\mathcal{M}$. If $\mathcal{M}$ has minimal rank six, then the factor module $\mathcal{M}' = \mathcal{M}/\mathcal{M}_p$ is finite. This implies (see last section) that each icosahedrally symmetric module of minimal rank can be viewed as a centering of $\mathcal{M}_p$. It has been shown [RMW] that in addition to $\mathcal{M}_p$ there are two different centerings. One of them, $\mathcal{M}_f$, can be obtained as the Z-span of the vectors in an orbit of the icosahedral group. As a starting vector we have to choose the sum of two of the basis vectors of $\mathcal{M}_p$ described above. Clearly, such a starting vector is invariant under a twofold rotation, so that we obtain an orbit of 30 vectors, of which however only six are rationally independent. Since each of the vectors in this orbit is a sum or difference of two basis vectors of $\mathcal{M}_p$, $\mathcal{M}_f$ consists precisely of those vectors of $\mathcal{M}_p$ for which $\sum n_i = even$, where the indices n_i refer to the basis of $\mathcal{M}_p$ introduced above.

The other centering cannot be obtained as the Z-span of vectors in a single orbit of the icosahedral group. This is not easy to see by working in three dimensions only. If we choose as starting vector one which is invariant under a threefold rotation, we obtain again a primitive module, but if we choose a vector in a general direction the situation becomes rather complicated. Therefore, we will describe this module in more detail only after lifting $\mathcal{M}_p$ to the six-dimensional icosahedral lattice. The lattice associated with $\mathcal{M}_b$ is then much easier to understand. For the moment we mention only that $\mathcal{M}_b$ consists of those vectors of $\mathcal{M}_p$ for which either all n_i are even or all n_i are odd.

Let us now determine with which representation the icosahedral group acts on the six-dimensional lattices. From the character table of I (see e. g. [KN]) we see that in order to obtain only integer characters the natural representation of I acting on physical space has to be equipped with the second, inequivalent 3d representation of I. Since this yields already dimension six we have determined the unique representation with the required properties. The primitive icosahedral lattice L_p can now be obtained as follows. First we choose a vector invariant under a C_5 subgroup of I. Each C_5 invariant subspace has dimension two and contains one direction in physical space and one in its orthogonal complement. In order to obtain a lattice, we have to choose the starting vector with non-vanishing components in both physical space and its complement. The length of these two components, $a_\parallel$ and $a_\perp$, will serve as our lattice parameters. On this starting vector, we act with the icosahedral group and then take the Z-span.

The two centerings, $\mathcal{M}_f$ and $\mathcal{M}_b$, naturally lift to sublattices of L_p, L_f and L_b, which both are centerings of L_p. That there are no other icosahedral lattices can be seen by a comparison with the complete classification of six-dimensional lattices by Plesken and Hanrath [PH]. Other icosahedral lattices would have to be in the same crystal family, LXXXVII [PH], which contains however only the three icosahedral lattices we already know.

Again, one of the two parameters, $a_\perp$, is non-physical, and we can choose it to our convenience. If we set $a_\parallel = a_\perp$, L_p degenerates to a primitive hypercubic lattice, L_f and L_b to what one might call face centered and body centered hypercubic lattices, in analogy to three dimensions. The latter two are obtained by adding lattice points at the centers of all two-dimensional facets or six-dimensional hypercubes of L_p. Therefore, L_f and L_b will be called face centered icosahedral and body centered icosahedral respectively. The three cubic lattices obtained from icosahedral ones are the only cubic lattices and form together crystal family XCI [PH]. Of course, not the full cubic group is of physical relevance, but only its icosahedral subgroup. The embedding of the icosahedral group in the cubic group is easily derived. The cubic group consists of all signed permutations of the six vectors of the standard basis.

On the other hand, all elements of I can be viewed as signed permutations of the six pairs of opposite vertices of an icosahedron. If physical space $E^{\parallel}$ is embedded such that the standard basis vectors of the hypercubic lattice, together with their negatives, project onto the twelve vectors pointing to the vertices of an icosahedron, we have obtained a natural embedding of the icosahedral group in the cubic group. Since there is a unique representation of the icosahedral group which is the symmetry group of a lattice and leaves a 3-dimensional subspace invariant, it must coincide with the one constructed above.

Let us now return to the special case of L_b. To understand this lattice we first note that [K1,K2] in L_p there are two inequivalent positions with full icosahedral symmetry, namely the lattice points and the centers of the six-dimensional hypercubes. Since the icosahedral symmetry does not mix these two classes of points, they can be occupied independently of each other. If only one class is occupied, the primitive lattice is obtained. If however both classes are occupied then the points in the two classes become equivalent, and it is easy to check that we obtain indeed a lattic, L_b.

That L_b cannot be generated by vectors in a single orbit of the icosahedral group can be seen as follows. Each basis of L_b must certainly contain at least one of the vectors $(\pm 1, \pm 1, \pm 1, \pm 1, \pm 1, \pm 1)$. The set of all these vectors decays into four orbits of the icosahedral group, two of size 12 and two of size 20. The vecors in the smaller orbits are invariant under a fivefold rotation each, those in the larger orbits under a threefold rotation. Therefore, each orbit generates only a primitive lattice, and at least two orbits are required for the generation of L_b.

2.4 Selfsimilarity Properties

The lattices we have discussed in the preceeding sections have additional "symmetries" relevant for quasicrystals. By these we mean certain elements of the normalizers of the Bravais groups of these lattices in $GL_n(Z)$. Recall that the normalizer N of G in $GL_n(Z)$ consists of all elements n of $GL_n(Z)$ which commute with G, i. e. for which $nGn^{-1} = G$. Elements of the normalizer map each orbit under G onto a full orbit. The normalizers of all the Bravais groups discussed above are infinite: they contain free Abelian subgroups. Particularly interesting for quasicrystals are those elements of the normalizer which generate such a free subgroup and leave in addition both $E^{\parallel}$ and $E^{\perp}$ separately invariant. Those elements n which moreover have the property that $n|_{E^{\parallel}} \geq 1$ and $n|_{E^{\perp}} \leq 1$ can be related to inflation and deflation transformations of quasiperiodic tilings based on these lattices, and to certain scaling properties of the Fourier spectrum of a quasicrystal. It is these elements of the normalizer which will be discussed in the following.

Let us first describe these additional symmetries and then explain their appli-

cations. We express them in terms of an appropriately chosen lattice basis. This lattice basis is uniquely determined if we specify the projections of the basis vectors onto physical space, i. e. the basis of the frequency module $\mathcal{M}$. For the octagonal primitive, decagonal and dodecagonal Bravais classes, we choose

$$\begin{aligned} \mathbf{e}_i^{\parallel} &= (a_{\parallel}\cos(\tfrac{2\pi i}{p}), a_{\parallel}\sin(\tfrac{2\pi i}{p}), 0), \qquad i = 1, \ldots, 4 \\ \mathbf{e}_5^{\parallel} &= (0, 0, c), \end{aligned} \tag{2.4}$$

where p=8, 10 or 12. Since the pentagonal and the octagonal centered Bravais classes are centerings of the decagonal and octagonal primitive Bravais classes respectively, they are generated by

$$\mathbf{e}_i^{\parallel} = (a_{\parallel}\cos(\tfrac{2\pi i}{p}), a_{\parallel}\sin(\tfrac{2\pi i}{p}), c), \qquad i = 1, \ldots, 5, \quad p = 5 \text{ or } 8. \tag{2.5}$$

Since a selfsimilarity transformation M is in $GL_n(Z)$ and commutes with G, the (periodic) z-direction must be an eigenvector of M with eigenvalue ± 1. Since M maps G-orbits onto G-orbits, in the quasiperiodic plane M must act like a change of scale, possibly followed by a rotation. Moreover, M must be in $GL_n(Z)$, i. e. it must be invertible in the integers. This restricts the possible changes of scale dramatically. In particular, this condition implies that if M stretches the quasiperiodic plane by a factor λ, the orthogonal space $E^{\perp}$ must be stretched by a factor λ^{-1} (note that since M commutes with G these two spaces must have constant stretching factors). For instance, in the octagonal case, if we do not change the main lattice axis, λ must be of the form $\lambda = n + m\sqrt{2}$, and consequently (2.3) $\lambda^{-1} = n - m\sqrt{2}$, which implies $\lambda = 1 + \sqrt{2}$ or integer powers thereof. For the other Bravais classes, similar conditions can be derived, and then it is easy to determine the matrices M. We obtain

$$M_5 = \begin{pmatrix} 1 & 0 & -1 & -1 & 0 \\ 0 & 1 & 0 & -1 & -1 \\ -1 & 0 & 1 & 0 & -1 \\ -1 & -1 & 0 & 1 & 0 \\ 0 & -1 & -1 & 0 & 1 \end{pmatrix}, \qquad \lambda_5 = \tau^2 = \tau + 1 = \frac{1}{2}(3 + \sqrt{5}), \tag{2.6}$$

$$M_8 = \begin{pmatrix} 1 & 1 & 0 & -1 & 0 \\ 1 & 1 & 1 & 0 & 0 \\ 0 & 1 & 1 & 1 & 0 \\ -1 & 0 & 1 & 1 & 0 \\ 0 & 0 & 0 & 0 & 1 \end{pmatrix}, \qquad \lambda_8 = 1 + \sqrt{2}, \tag{2.7}$$

$$M_8' = \begin{pmatrix} 1 & 0 & -1 & -1 & 0 \\ 1 & 1 & 1 & 0 & -1 \\ 0 & 1 & 1 & 1 & 0 \\ -1 & 0 & 1 & 1 & 1 \\ 0 & -1 & -1 & 0 & 1 \end{pmatrix}, \qquad \lambda_8' = 1 + \sqrt{2}, \tag{2.8}$$

$$M_{10} = \begin{pmatrix} 1 & 1 & 0 & -1 & 0 \\ 0 & 0 & 1 & 1 & 0 \\ 1 & 1 & 0 & 0 & 0 \\ -1 & 0 & 1 & 1 & 0 \\ 0 & 0 & 0 & 0 & 1 \end{pmatrix}, \qquad \lambda_{10} = \tau = \frac{1}{2}(1+\sqrt{5}). \tag{2.9}$$

$$M_{12}^{(1)} = \begin{pmatrix} 2 & 1 & 0 & -1 & 0 \\ 2 & 2 & 1 & 0 & 0 \\ 0 & 1 & 2 & 2 & 0 \\ -1 & 0 & 1 & 2 & 0 \\ 0 & 0 & 0 & 0 & 1 \end{pmatrix}, \qquad \lambda_{12}^{(1)} = 2+\sqrt{3}, \tag{2.10}$$

$$M_{12}^{(2)} = \begin{pmatrix} 1 & 0 & 0 & -1 & 0 \\ 1 & 1 & 0 & 0 & 0 \\ 0 & 1 & 1 & 1 & 0 \\ 0 & 0 & 1 & 1 & 0 \\ 0 & 0 & 0 & 0 & 0 \end{pmatrix}, \qquad \lambda_{12}^{(2)} = \sqrt{2+\sqrt{3}}, \tag{2.11}$$

We see that in the dodecagonal case we have two generators and in the other cases just one. However, the square of $M_{12}^{(2)}$ differs from $M_{12}^{(1)}$ only by an element of the Bravais group ($M_{12}^{(1)}$ stretches by a factor $\sqrt{2+\sqrt{3}}$ and then rotates by 15°).

The list of generators given above is complete. Since the z-direction is an eigendirection of eigenvalue ± 1 of the mapping M, for the primitive lattices this follows from a comparison with the presentation of the normalizers of the octagonal, decagonal and dodecagonal Bravais groups in four dimensions given in [Br]. For the non-primitive lattices we note that the z=0 plane is the projection of a 4-dimensional octagonal or decagonal lattice, and that because of the eigenvalue ± 1 in z-direction M must transform these points among themselves. Therefore, the group of selfsimilarity transformations for a non-primitive lattice is a subgroup of that of the corresponding primitive one. For the octagonal non-primitive lattice, we obtain the same group as for the octagonal primitive lattice, but for the pentagonal lattice the group of selfsimilarity operations is a subgroup of index two of that of the decagonal lattice.

The basis vectors generating the primitive icosahedral frequency module are given by

$$\begin{aligned} \mathbf{e}_1^{\parallel} &= a_{\parallel}(0,0,1), \\ \mathbf{e}_i^{\parallel} &= \tfrac{a_{\parallel}}{\sqrt{5}}(2\cos(\tfrac{2\pi i}{5}), 2\sin(\tfrac{2\pi i}{5}), 1), \qquad i = 2, \ldots, 6. \end{aligned} \tag{2.12}$$

The projections of the corresponding basis vectors of the primitive icosahedral lattice onto $E^{\perp}$ are given by

$$\begin{aligned} \mathbf{e}_1^{\perp} &= a_{\perp}(0,0,-1), \\ \mathbf{e}_i^{\perp} &= \tfrac{a_{\perp}}{\sqrt{5}}(2\cos(\tfrac{4\pi i}{5}), 2\sin(\tfrac{4\pi i}{5}), 1). \end{aligned} \tag{2.13}$$

Therefore, the scale change factor λ must be of the form $n + m\sqrt{5}$, and its inverse is then $-n + m\sqrt{5}$, from which it follows that $\lambda = 2 + \sqrt{5} = \tau^3$. The matrix of the corresponding mapping reads

$$M = \begin{pmatrix} 2 & 1 & 1 & 1 & 1 & 1 \\ 1 & 2 & 1 & -1 & -1 & 1 \\ 1 & 1 & 2 & 1 & -1 & -1 \\ 1 & -1 & 1 & 2 & 1 & -1 \\ 1 & -1 & -1 & 1 & 2 & 1 \\ 1 & 1 & -1 & -1 & 1 & 2 \end{pmatrix}, \quad \lambda = 2 + \sqrt{5}. \tag{2.14}$$

Since M leaves invariant also the two subsets of the primitive icosahedral lattice L_p corresponding to the two centerings of L_p, L_f and L_b, given by the conditions $\sum n_i = even$ (L_f) and all $n_i = even$ or all $n_i = odd$ (L_b), the mapping M is also a selfsimilarity operation for these lattices. However, for the two centered lattices the group of transformations generated by M is only a subgroup of index three of the whole group of selfsimilarity transformations, the generator of which has been determined by Elser [E2]. This generator is given by

$$M' = \frac{1}{2} \begin{pmatrix} 1 & 1 & 1 & 1 & 1 & 1 \\ 1 & 1 & 1 & -1 & -1 & 1 \\ 1 & 1 & 1 & 1 & -1 & -1 \\ 1 & -1 & 1 & 1 & 1 & -1 \\ 1 & -1 & -1 & 1 & 1 & 1 \\ 1 & 1 & -1 & -1 & 1 & 1 \end{pmatrix}, \quad \lambda' = \tau, \tag{2.15}$$

where we have used the same basis as for the primitive lattice L_p. It is easy to verify that M' maps lattice points of L_f or L_b onto lattice points, although M' has non-integer entries, which comes simply from the fact that we didn't use a lattice basis of L_f or L_b. Note that the relation $\lambda = \lambda'^3$ holds also for the matrices, $M = M'^3$.

Let us now turn to the applications. In chapter 1 we have considered quasiperiodic tilings whose vertices are the projections of the lattice points $\mathbf{x} \in L$ which are contained in a strip $S = C \times E^{\parallel}$, where $C \subset E^{\perp}$ is an open domain with compact closure. Here we use for L one of the lattices with crystallographically forbidden point group discussed above, $E^{\parallel}$ is an invariant subspace of this symmetry, and C is supposed to be invariant under the point group of L. Furthermore we assume that there exists an open domain $D \subset C$ such that every point $x \in C$ can be connected to every point $y \in D$ by a straight line which is completely contained in C, i. e. we require C to be star-shaped. In the following D is supposed to be the largest such domain.

The lattices discussed above all admit a free group of selfsimilarity transformations whose generator M satisfies $M|_{E^{\perp}} = \lambda^{-1} \cdot 1$.* Choose the origin of L such

*Operations generated by $M_{12}^{(2)}$ do not belong to this class and need a special treatment, see below.

that its projection onto $E^\perp$ falls into the domain D, and let us compare pattern A based on acceptance region C, and pattern B, based on MC. Since the projection onto $E^\parallel$ commutes with M, there are two ways to go from A to B. Pattern B can be obtained from A by first applying M to all lattice points of L inside $C \times E^\parallel$ and then projecting them onto $E^\parallel$. Since C is star-shaped, $MC \subset C$, and so the pattern obtained in this way is a subset of A. Moreover, since M is a lattice automorphism, the mapping

$$M : L \cap (C \times E^\parallel) \to L \cap (MC \times E^\parallel) \tag{2.16}$$

is onto and so we indeed obtain pattern B. Alternatively, we can first project all lattice points in $C \times E^\parallel$ onto $E^\parallel$ and then apply M. This amounts just to scaling pattern A by a factor λ in all quasiperiodic directions, which again yields pattern B. Therefore we find that pattern A scaled by a factor λ in all quasiperiodic directions is a subset of A. Of course, for the origin of this scaling we can use any vertex of the pattern which is the projection of a lattice point contained in $D \times E^\parallel$. If C is convex, this is the case for all vertices of the tiling.

If we would like to use $M_{12}^{(2)}$ for selfsimilarity, we have to impose stronger conditions on C in order that $MC \subset C$. In this case, it is sufficient to require that C is not only 12-fold symmetric, but even 24-fold symmetric (and star-shaped), or that C is convex. In more complicated examples, when there occur different eigenvalues ≤ 1 in $M|_{E^\perp}$, even more care is needed. Then, even a convex acceptance domain is in general not sufficient to ensure the existence of an open domain into which the origin of the scaling may fall. Particular difficulties have to be overcome also in the case of the Penrose pattern, for which M_5 is the relevant selfsimilarity operation. Since M_5 changes the scale by powers of τ^2, the classical inflation and deflation operations for the Penrose pattern, which change the scale by a factor τ, cannot be of this form. In general, in a Penrose pattern there is no vertex around which it is invariant under a change of scale by τ. Only in the two exactly fivefold symmetric Penrose patterns exists such a vertex (the center). A more detailed discussion is postponed to chapter 4, where also the construction of Penrose patterns is discussed.

These selfsimilarity operations can be applied to reciprocal space as well. Elser [E2] has used the scaling of the intensity of a sequence of peaks obtained by iterating M for the determination of the lattice constant of L.

Chapter Three
Space Groups for Quasicrystals

3.1 Introduction

A quasicrystal is an aperiodic structure with, in general, no symmetry (in real space) at all. But since it is the restriction of a higherdimensional periodic structure to physical space, we can nevertheless associate a space group with it, namely that of the periodic structure. The space group symmetry of the periodic structure is reflected in the (experimentally observable) intensities of the Fourier spectrum of the quasicrystal. These intensities are invariant under the point group belonging to the space group, and a non-symmorphic space group (one which is not the semi-direct product of the point group with the lattice of translations) can lead to characteristic extinctions in the Fourier spectrum. However, quasicrystals with two different space groups cannot always be distinguished by the symmetry of the intensities of their Fourier spectrum and the set of systematic extinctions. For instance, the intensities of the Fourier spectrum are always inversion symmetric (Friedel's law), whether or not inversion symmetry is part of the point group, and two different space groups may lead to the same set of characteristic extinctions. This is of course the same as for ordinary threedimensional crystals, where the 230 proper space group types fall into 122 so called Laue classes which can be distinguished by their diffraction pattern.

In this chapter, we derive a complete list of space groups for the five (2+1)-reducible Bravais classes discussed in chapter two, and for each of these space groups we determine the extinction pattern. For icosahedral symmetry, the list of space groups is already known [J2, LR], and the extinction patterns have been determined [LR]. Therefore, we confine ourselves to the (2+1)-reducible case. Most recently, these space groups have independently been obtained also by Janssen [J3].

In a first step, for each of the five Bravais classes we have to determine its point groups. To do so we choose a lattice basis and express the full point group of the lattice in terms of this basis. In this lattice basis, the point group becomes a finite subgroup B of $GL_n(Z)$ and is called the *Bravais group* of the lattice. We then have to find all subgroups of B which are not subgroup of any other Bravais group of smaller order. For the Bravais groups we are interested in this means simply that the point group G still contains an element of order at least 5. Two point groups are considered as equivalent iff they are conjugated subgroups of $GL_n(Z)$.

The determination of all point groups is greatly simplified if we note that for each of the five quasicrystal Bravais classes under consideration there exists a three

dimensional Bravais class such that the two corresponding Bravais groups have a very similar structure. The dodecagonal and octagonal primitive Bravais classes correspond to the tetragonal primitive Bravais class, the octagonal centered to the tetragonal C-centered, the decagonal to the hexagonal (primitive) and the pentagonal to the hexagonal R-centered Bravais classes [Br]. It turns out that for each such pair of a five dimensional and a three dimensional Bravais class the number of point groups is the same, and the structure of these point group is completely analogous — there is a natural one-to-one correspondence between the two sets of point groups. The key observation is that 12 and 8 as well as 4 (the order of the highest order element of the tetragonal group) are divisible by 4, whereas 10 and 6 are not. This is the reason why the octagonal and dodecagonal Bravais classes are related to the tetragonal ones, and the pentagonal and decagonal Bravais classes to the hexagonal ones (note that hexagonal R-centered lattice is only 3-fold symmetric). Since the three dimensional point groups are tabulated in [Br], the necessary quasicrystal point groups are easy to determine.

Next, for each point group G we have to find the space groups belonging to it. In order to do this we choose a set of generators $A, B, \dots$ for G, and a set of relations $f_i(A, B, \dots) = 1$ defining G. A space group Γ belonging to point group G is then generated by all elements of the Euclidean group $E(n)$ of the form $(X, x+t)$, where X is a generator of G, x is a (fixed) so called *non-primitive translation vector* associated with X, and t is any lattice vector. The non-primitive translations, defined up to a lattice vector, are subject to the conditions that for each defining relation $f_i(A, B, \dots) = 1$ we have

$$f_i\left((A, a), (B, b), \dots\right) = (1, t), \tag{3.1}$$

where t is any lattice vector. The space group is therefore determined by the set of non-primitive translations. Not every set of non-primitive translations satisfying (3.1) defines a distinct space group however. There are two kinds of equivalence relations. The first is conjugation by elements of $GL_n(Z)$, i. e. the space group does not depend on the choice of lattice basis. Since we are working with a fixed representative in each conjugation class of point groups, we can restrict ourselves to conjugation with elements in the normalizer N of G in $GL_n(Z)$ (the normalizer contains those elements which commute with G). This equivalence leads only in the dodecagonal case to a non-trivial result. It is however very important in the icosahedral case [LR]. For the three primitive lattices the normalizers can be deduced from those of the corresponding four-dimensional lattices, which are listed in [Br].

More important is the freedom of choosing the origin. Most of the different solutions of (3.1) just correspond to different choices of the origin. In order to avoid this ambiguity we fix the origin as far as possible. In the set of generators of each

point group, there is always a unique element of order at least 5. This element is a rotation around the z-axis, and is denoted by A or A', or, if it is followed by an inversion, by $\bar{A}$ or $\bar{A}'$. If the order of A (or A' etc.) is n, the relation

$$(A, a)^n = (A^n, A^{n-1}a + A^{n-2}a + \cdots + a) = (1, t) \tag{3.2}$$

must hold, with t a lattice vector. This is a condition only on the z-component of a. However, we are free to choose the origin to our convenience. We choose the origin such that a points in the direction of a lattice vector with smallest possible z-component. For the three primitive lattices, we can choose the origin such that a is parallel to the z-axis. Since this choice of origin greatly simplifies the whole analysis, we shall adopt it throughout this chapter. Still, we are free to shift the origin in z-direction, which does not affect the value of a. We can use this freedom to force components of other non-primitive translations to zero. For instance, if the central inversion $C = -1$ is present, we choose the z-component of the associated non-primitive translation equal to zero. If C is not present, but $\bar{A}$ instead, we can make the z-component of a vanish. Finally, if neither of this is the case, but we have a mirror $\bar{B}$ which inverts also the z-direction, we choose $b_z = 0$.

For the following analysis, it is sometimes convenient to adopt the following notation. With respect to an orthonormal basis, the generators of G can be written in block diagonal form:

$$X = \begin{pmatrix} \vec{X} & 0 \\ 0 & X_z \end{pmatrix}, \tag{3.3}$$

where $\vec{X}$ is a 4×4-block, and $X_z = \pm 1$. Similarly, we decompose a non-primitive translation vector as $x = (\vec{x}, x_z)$. This notation will allow us to make statements about the z-components of non-primitive translations alone, or about the components in the orthogonal complement of the z-axis.

Let us now turn to the consequences a non-symmorphic space group symmetry has on the Fourier spectrum. If the higherdimensional structure $\rho(r)$ is invariant under the space group element (X, x), we have $\rho(r) = \rho(Xr + x)$ and hence

$$\hat{\rho}(k) = e^{ik\cdot x}\hat{\rho}(X^{-1}k). \tag{3.4}$$

Now, if for a given k

$$e^{ik\cdot x} \neq 1 \quad \text{and} \quad \hat{\rho}(k) = \hat{\rho}(X^{-1}k), \tag{3.5}$$

then $\hat{\rho}(k)$ must necessarily vanish. The latter condition is satisfied if either $k = X^{-1}k$ or if there is a space group element $(Y, 0)$ with vanishing translation component mapping k to $X^{-1}k$. However, if such an element $(Y, 0)$ exists, we can apply

our arguments to (XY^{-1}, x), whose linear part leaves k invariant. Therefore, it is sufficient to search for space group elements (X, x) for which $X^{-1}k = k$. Summarizing, a peak indexed by a reciprocal lattice vector k is extinct iff there exists a space group element (X, x) such that $X^{-1}k = k$ and $e^{ik\cdot x} \neq 1$.

Let us illustrate this with two examples. First we assume the existence of a screw axis $(A, \frac{1}{n}e_z)$, where A is a rotation around the z-axis, and e_z is the shortest lattice vector parallel to the z-axis. The k-vectors invariant under A are those parallel to the z-axis. Therefore, the peaks on the z-axis vanish unless $k \cdot \frac{1}{n}e_z$ is a multiple of 2π. If $k = m\hat{e}_z$, where $\hat{e}_z$ is the shortest k-vector in z-direction, this is the case iff $\frac{m}{n} \in Z$, i. e. on the z-axis only every n^{th} peak is present. Next, let us assume a mirror glide plane containing the z-axis. The non-primitive translation is again $\frac{1}{n}e_z$. This glide plane causes extinctions of those peaks k in the mirror plane for which $k \cdot \frac{1}{n}e_z$ is not a multiple of 2π. Hence, in the mirror plane, in z-direction only every n^{th} layer of peaks is present.

In the rest of this chapter we tabulate the space groups for the five Bravais classes. We obtain a total of 187 *proper space groups*. For proper space groups basis with positive and negative orientations are considered as inequivalent. If we consider basis with positive and negative orientaions as equivalent however, certain pairs of proper space groups, so called enantiomorphic pairs, fall together, so that only 152 space groups remain. In the following, we will stick to proper space groups. In each case, we comment on the interesting points in the derivation, but do not supply all the details. Moreover, for each space group we derive the systematic extinctions. Throughout the rest of this chapter we use the lattice basis (2.4) or (2.5) introduced in the last chapter. This holds also for the basis of the reciprocal lattices (with different lattice parameters however). This means that in general for the reciprocal lattice we are not using the basis dual to that of the real space lattice.

3.2 Space Groups in the Dodecagonal Bravais Class

In the basis (2.4) the generators of the dodecagonal Bravais group and its relevant subgroups are

$$A = \begin{pmatrix} 0 & 0 & 0 & -1 & 0 \\ 1 & 0 & 0 & 0 & 0 \\ 0 & 1 & 0 & 1 & 0 \\ 0 & 0 & 1 & 0 & 0 \\ 0 & 0 & 0 & 0 & 1 \end{pmatrix}, \quad B = \begin{pmatrix} 0 & 0 & 0 & 1 & 0 \\ 0 & 0 & 1 & 0 & 0 \\ 0 & 1 & 0 & 0 & 0 \\ 1 & 0 & 0 & 0 & 0 \\ 0 & 0 & 0 & 0 & 1 \end{pmatrix}, \tag{3.6}$$

as well as $C = -1$, $\bar{A} = CA$, $\bar{B} = CB$. The defining relations are

$$A^{12} = B^2 = C^2 = BABA = 1, \quad [A, C] = [B, C] = 0. \tag{3.7}$$

Let us now derive the relations for the non-primitive translations following from (3.1). All these relations will always be understood modulo lattice vectors. The origin we choose as explained earlier. If C is present, we choose $c_z = 0$; then from (3.6) it follows that $Ac = c$, which implies $c = 0$. If B or $\bar{B}$ is present, we have $\vec{B}\vec{b} + \vec{b} = 0$ and $\vec{B}\vec{A}\vec{b} + \vec{b} = 0$ which together imply $\vec{b} = 0$. Let us now turn to the z-components. If A is present, we clearly have $12a_z \in L$. If, in addition, C is present, we even have $-a_z = a_z$, so that $2a_z \in L$. The relation $B^2 = 1$ implies $2b_z \in L$, and $BABA = 1$ implies $2b_z + 2a_z \in L$. Putting all this together, we arrive at the following table of space groups:

Table 3.1: Space groups in the dodecagonal Bravais class

Point group	Gener.	Non-primitive translations	n	Ext. pattern
12	A	$a = (0,0,0,0,\frac{p}{12})$	12	$2,4,6,12$
$\overline{12}$	$\overline{A}$		1	
$12/m$	A, C	$a = (0,0,0,0,\frac{p}{2})$	2	2
$12\,m\,m$	A, B	$a = (0,0,0,0,\frac{p}{2})$ $b = (0,0,0,0,\frac{m}{2})$	3*	m, mm
$12\,2\,2$	$A, \overline{B}$	$a = (0,0,0,0,\frac{p}{12})$	12	$2,4,6,12$
$\overline{12}\,2\,m$	$\overline{A}, B$	$b = (0,0,0,0,\frac{m}{2})$	2	m
$\overline{12}\,m\,2$	$\overline{A}, \overline{B}$	$b = (0,0,0,0,\frac{m}{2})$	2	m
$12/m\,m\,m$	A, B, C	$a = (0,0,0,0,\frac{p}{2})$ $b = (0,0,0,0,\frac{m}{2})$	3*	m, mm

*(p=0, m=1) and (p=1, m=0) are equivalent, see text

If both A and B are present, the application of the relations stated above yields a pair of equivalent space groups, the equivalence relation being conjugation by the selfsimilarity mapping $M_{12}^{(2)}$ (2.11). In this case, the point group contains two inequivalent sets of mirror planes. The representative of one set, m is left invariant by B, that of the other set, m', is left invariant by AB. Any of these sets of mirrors in the point group can be a set of true mirror planes or of glide mirror planes in the space group. However, if one set consists of true mirrors, the other of glide mirrors, one cannot say which is which — conjugation by $M_{12}^{(2)}$ simply exchanges the two sets.

In table 3.1 we have included symbols for the possible extinction patterns which occur with each point group. A symbol n, n a positive natural number, indicates that on the z-axis only every n^{th} peak is present. These extinctions originate from a screw axis in the space group. A symbol m means that in one set of mirror planes of the point group peaks with odd z-index are absent, whereas the symbol mm implies that this is the case for both sets of mirrors. These exinctions are due to mirror glide planes. From the examples in last section it is obvious which extinction pattern belongs to which space group.

3.3 Space Groups in the Octagonal Primitive Bravais Class

For point groups in the octagonal primitive Bravais class, we use the generators

$$A = \begin{pmatrix} 0 & 0 & 0 & -1 & 0 \\ 1 & 0 & 0 & 0 & 0 \\ 0 & 1 & 0 & 0 & 0 \\ 0 & 0 & 1 & 0 & 0 \\ 0 & 0 & 0 & 0 & 1 \end{pmatrix}, \quad B = \begin{pmatrix} 0 & 1 & 0 & 0 & 0 \\ 1 & 0 & 0 & 0 & 0 \\ 0 & 0 & 0 & -1 & 0 \\ 0 & 0 & -1 & 0 & 0 \\ 0 & 0 & 0 & 0 & 1 \end{pmatrix}, \tag{3.8}$$

and $C = -1$, $\bar{A} = CA$, $\bar{B} = CB$ in the basis (2.4). These generators satisfy the relations

$$A^8 = B^2 = C^2 = BABA = 1, \quad [A, C] = [B, C] = 0. \tag{3.9}$$

Hence, apart from the order of A, the point group is very similar to that of the dodecagonal Bravais class. If C is present, we again choose $c_z = 0$. In contrast to the dodecagonal case however, from $Ac = c$ we cannot conclude that c vanishes: a second solution is $c = (\frac{1}{2}, \frac{1}{2}, \frac{1}{2}, \frac{1}{2}, 0)$. For the non-primitive translation b the situation is similar: we obtain $\vec{b} = (\frac{n}{2}, \frac{n}{2}, \frac{n}{2}, \frac{n}{2})$, $n = 0, 1$. In the five Bravais classes, $\vec{b}$ and $\vec{c}$ are the only occurrences of non-primitive translations parallel to quasiperiodic directions. Such a non-primitive translation $\vec{b}$ occurs also in the octagonal Bravais class in four dimensions [Br], where it gives rise to the only non-symmorphic space group in the octagonal, decagonal and dodecagonal Bravais classes in four dimensions. For the z-components of the non-primitive translations, the situation is the same as that in the dodecagonal case, so that we arrive at the space groups listed in table 3.2.

Table 3.2: Space groups in the octagonal primitive Bravais class

Point group	Gener.	Non-primitive translations	n	Ext. pattern
8	A	$a = (0, 0, 0, 0, \frac{p}{8})$	8	$2, 4, 8$
$\overline{8}$	$\overline{A}$		1	
$8/m$	A, C	$a = (0, 0, 0, 0, \frac{p}{2})$ $c = (\frac{q}{2}, \frac{q}{2}, \frac{q}{2}, \frac{q}{2}, 0)$	4	$2, c, 2 + c$
$8\,m\,m$	A, B	$a = (0, 0, 0, 0, \frac{p}{2})$ $b = (\frac{n}{2}, \frac{n}{2}, \frac{n}{2}, \frac{n}{2}, \frac{m}{2})$	8	$m, m', mm, s,$ $s', m + s, m + s'$
$8\,2\,2$	$A, \overline{B}$	$a = (0, 0, 0, 0, \frac{p}{8})$ $b = (\frac{n}{2}, \frac{n}{2}, \frac{n}{2}, \frac{n}{2}, 0)$	16	$k, b, k + b$ $k = 2, 4, 8$
$\overline{8}\,2\,m$	$\overline{A}, B$	$b = (\frac{n}{2}, \frac{n}{2}, \frac{n}{2}, \frac{n}{2}, \frac{m}{2})$	4	$m, b, m + b$
$\overline{8}\,m\,2$	$\overline{A}, \overline{B}$	$b = (\frac{n}{2}, \frac{n}{2}, \frac{n}{2}, \frac{n}{2}, \frac{m}{2})$	4	m', s, s'
$8/m\,m\,m$	A, B, C	$a = (0, 0, 0, 0, \frac{p}{2})$ $b = (\frac{n}{2}, \frac{n}{2}, \frac{n}{2}, \frac{n}{2}, \frac{m}{2})$ $c = (\frac{q}{2}, \frac{q}{2}, \frac{q}{2}, \frac{q}{2}, 0)$	16	$c, m, m', mm, s,$ $s', m + s, m + s'$ $x + c$

Because of the presence of nonprimitive translations parallel to quasiperiodic directions, the exinction patterns are more complicated than in the other cases. If $n = 0$ and $q = 0$, the situation is very similar to the dodecagonal case. Again there

are two sets of inequivalent mirror planes, represented by m and m', which both can be glide mirror planes or true mirror planes. The two representatives are left invariant by B and AB respectively. However, in contrast to the dodecagonal case, there is no element in the normalizer of the Bravais group or of one of its point groups, a conjugation with which would interchange the two sets. Hence these two sets can be distinguished. If only one of these sets consists of glide planes, one can determine which one it is. Therefore, we have to distinguish the two symbols for the extinction pattern, m and m'.

If $n = 1$ or $q = 1$, the situation is more complicated. The generator A^4C leaves all directions except the z-axis invariant and has the same non-primitive translation as C. Therefore, if $q = 1$, in the plane $z = 0$ all peaks for which the sum of the indices is odd are extinct. We denote this with the symbol c. Next we consider the extinctions caused by the translation b. These extinctions must be located either in a plane of type m, or in a plane of type m'. Since for all peaks in a plane of type m we have $\sum_{i=1}^{4} k_i = even$, the non-primitive translation $b = (\frac{1}{2}, \frac{1}{2}, \frac{1}{2}, \frac{1}{2}, 0)$ cannot cause any extinctions in this plane. In the planes of type m', the situation is different. We illustrate this with the plane left invariant by AB, which contains the $\mathbf{e}_2$-direction. Peaks in this plane have index $(j, k, j, 0, \ell)$. A peak is therefore extinct whenever $(k \cdot n + \ell \cdot (m + p))$ is odd (note that the non-primitive translation associated with AB is $b = (\frac{1}{2}, \frac{1}{2}, \frac{1}{2}, \frac{1}{2}, \frac{m+p}{2})$). Two cases have to be distinguished. If $m + p$ is even, all layers in the planes of type m' carry the same extinction pattern s. If $m + p$ is odd, the extinction pattern depends on whether the z-coordinate of the layer is even or odd. This second extinction pattern with alternating layers in the m'-planes we denote by s'. Of course, both s and s' can be combined with extinction pattern m in the m-type planes. If ABC, but not C is present, and if $n = 1$, then in the m'-type layers all peaks with vanishing z-component and odd index are extinct. We denote this by the symbol b. For the point group $8/mmm$ we have used the symbol $x + c$, where x stands for any of the other extinction patterns occuring for this point group.

3.4 Space Groups in the Octagonal Centered Bravais class

The octagonal centered Bravais group is generated by

$$A = \begin{pmatrix} 0 & 0 & 0 & 0 & 1 \\ 1 & 0 & 0 & 0 & -1 \\ 0 & 1 & 0 & 0 & 0 \\ 0 & 0 & 1 & 0 & 0 \\ 0 & 0 & 0 & 1 & 1 \end{pmatrix}, \quad B = \begin{pmatrix} 0 & 1 & 1 & 1 & 1 \\ 1 & 0 & 0 & 0 & -1 \\ 0 & 0 & 0 & -1 & 0 \\ 0 & 0 & -1 & 0 & 0 \\ 0 & 0 & 1 & 1 & 1 \end{pmatrix}. \tag{3.10}$$

and $C = -1$. For some point groups we again need $\bar{A} = CA$ and $\bar{B} = CB$. The

defining relations are

$$A^8 = B^2 = C^2 = BABA = 1, \quad [A, C] = [B, C] = 0. \tag{3.11}$$

If A and B are present, we get $a = (\frac{p}{2}, 0, 0, 0, 0)$ and $b = (\frac{m+p}{2}, \frac{p}{2}, 0, 0, \frac{p}{2})$, whereas if $\bar{A}$ and B or $\bar{B}$ are present, we obtain $a = 0$ and $b = (\frac{m}{2}, 0, 0, 0, \frac{m}{2})$, $p, m = 0, 1$. Together with arguments similar to those in the previous sections, we obtain:

Table 3.3: Space groups in the octagonal centered Bravais class

Point group	Gener.	Non-primitive translations		n	Ext. pattern
8	A	$a = (\frac{p}{4}, 0, 0, 0, 0)$		4	$2, 4$
$\overline{8}$	$\overline{A}$			1	
$8/m$	A, C	$a = (\frac{p}{2}, 0, 0, 0, 0)$		2	2
$8\,m\,m$	A, B	$a = (\frac{p}{2}, 0, 0, 0, 0)$	$b = (\frac{m+p}{2}, \frac{p}{2}, 0, 0, \frac{m}{2})$	4	m, m', mm
$8\,2\,2$	$A, \overline{B}$	$a = (\frac{p}{4}, 0, 0, 0, 0)$		4	$2, 4$
$\overline{8}\,2\,m$	$\overline{A}, B$		$b = (\frac{m}{2}, 0, 0, 0, \frac{m}{2})$	2	m'
$\overline{8}\,m\,2$	$\overline{A}, \overline{B}$		$b = (\frac{m}{2}, 0, 0, 0, \frac{m}{2})$	2	
$8/m\,m\,m$	A, B, C	$a = (\frac{p}{2}, 0, 0, 0, 0)$	$b = (\frac{m+p}{2}, \frac{p}{2}, 0, 0, \frac{m}{2})$	4	m, m', mm

Some symbols for the extinction patterns have a somewhat different meaning than in the other cases. First we note that the reciprocal lattice is an octagonal centered lattice which is turned by $22,5°$ with respect to the real space lattice. Therefore, to a glide plane of type m belongs an extinction pattern m' (point group $\bar{8}\,2\,m$). For point group $\bar{8}\,m\,2$, the converse situation does not occur: the odd layers in the m'-type planes of the reciprocal lattice are absent altogether. For the point groups $8\,m\,m$ and $8/m\,m\,m$ a special situation occurs: if $m = 1$, then in the m' type layers of the reciprocal lattice only every second layer is present (symbol m'). If $p = 1$ however, in the m-type layers only every second layer is present. Since the m-planes contain only half the number of layers of the m'-planes, neighboring layers are four units apart in this case (symbol m). If both m and p are equal to one, we obtain the union of these two extinction patterns (symbol mm).

3.5 Space Groups in the Decagonal Bravais Class

In the decagonal Bravais class, we need the generators

$$A = \begin{pmatrix} 0 & 0 & 0 & -1 & 0 \\ 1 & 0 & 0 & 1 & 0 \\ 0 & 1 & 0 & -1 & 0 \\ 0 & 0 & 1 & 1 & 0 \\ 0 & 0 & 0 & 0 & 1 \end{pmatrix}, \quad B = \begin{pmatrix} 0 & 0 & 0 & 1 & 0 \\ 0 & 0 & 1 & 0 & 0 \\ 0 & 1 & 0 & 0 & 0 \\ 1 & 0 & 0 & 0 & 0 \\ 0 & 0 & 0 & 0 & 1 \end{pmatrix} \tag{3.12}$$

as well as $C = -1$, $A' = A^2$, $B' = AB$, $\bar{A} = CA$, $\bar{B} = CB$ and $\bar{B}' = CB'$. These

generators satisfy the relations

$$\begin{gathered} A^{10} = A'^5 = B^2 = B'^2 = C^2 = 1 \\ BABA = B'AB'A = BA'BA' = B'A'B'A' = 1 \\ [A, C] = [A', C] = [B, C] = [B', C] = 0. \end{gathered} \tag{3.13}$$

The relations $\vec{A}\vec{c} = \vec{c}$ and $\vec{A}'\vec{c} = \vec{c}$ both imply $\vec{c} = 0$, so that we have $c = 0$. From $\vec{B}\vec{b} + \vec{b} = 0$ and $\vec{B}\vec{A}\vec{b} + \vec{b} = 0$ we can deduce $\vec{b} = 0$. The same holds true if we replace A or B (or both) by A' or B' respectively. Note that we need only one of the generators B and B' each time, so that no ambiguity arises when we use the same symbol b for the non-primitive translations of both generators. The relations for the z-components of the non-primitive translations are very similar to those in the other primitive Bravais classes so that we need not repeat them here. The following table contains a list of all space groups in the decagonal Bravais class.

Table 3.4: Space groups in the decagonal Bravais class

Point group	Gener.	Non-primitive translations		n	Ext. pattern
5	A'	$a = (0,0,0,0,\frac{p}{5})$		5	5
5 1 2	$A', \overline{B}$	$a = (0,0,0,0,\frac{p}{5})$		5	5
5 2 1	$A', \overline{B'}$	$a = (0,0,0,0,\frac{p}{5})$		5	5
5 1 m	A', B		$b = (0,0,0,0,\frac{m}{2})$	2	m
5 m 1	A', B'		$b = (0,0,0,0,\frac{m}{2})$	2	m'
$\overline{5}$	$\overline{A'}$			1	
$\overline{5}$ 1 m	$\overline{A'}, B$		$b = (0,0,0,0,\frac{m}{2})$	2	m
$\overline{5}$ m 1	$\overline{A'}, B'$		$b = (0,0,0,0,\frac{m}{2})$	2	m'
10	A	$a = (0,0,0,0,\frac{p}{10})$		10	$2, 5, 10$
$\overline{10}$	$\overline{A}$			1	
$10/m$	A, C	$a = (0,0,0,0,\frac{p}{2})$		2	2
10 m m	A, B	$a = (0,0,0,0,\frac{p}{2})$	$b = (0,0,0,0,\frac{m}{2})$	4	m, m', mm
10 2 2	$A, \overline{B}$	$a = (0,0,0,0,\frac{p}{10})$		10	$2, 5, 10$
$\overline{10}$ 2 m	$\overline{A}, B$		$b = (0,0,0,0,\frac{m}{2})$	2	m
$\overline{10}$ m 2	$\overline{A}, \overline{B}$		$b = (0,0,0,0,\frac{m}{2})$	2	m'
$10/m$ m m	A, B, C	$a = (0,0,0,0,\frac{p}{2})$	$b = (0,0,0,0,\frac{m}{2})$	4	m, m', mm

The extinction pattern symbols are defined as in the previous paragraphs. The symbol m refers to the mirror B, m' to the mirror B'.

3.6 Space Groups in the Pentagonal Bravais Class

In the pentagonal Bravais class, we have to deal with the generators

$$A = \begin{pmatrix} 0 & 0 & 0 & 0 & 1 \\ 1 & 0 & 0 & 0 & 0 \\ 0 & 1 & 0 & 0 & 0 \\ 0 & 0 & 1 & 0 & 0 \\ 0 & 0 & 0 & 1 & 0 \end{pmatrix}, \quad B = \begin{pmatrix} 0 & 1 & 0 & 0 & 0 \\ 1 & 0 & 0 & 0 & 0 \\ 0 & 0 & 0 & 0 & 1 \\ 0 & 0 & 0 & 1 & 0 \\ 0 & 0 & 1 & 0 & 0 \end{pmatrix}, \tag{3.14}$$

and $C = -1$, $\bar{B} = CB$. The generators (3.14) satisfy the relations

$$A^5 = B^2 = C^2 = BABA = 1, \quad [A, C] = [B, C] = 0. \tag{3.15}$$

The relation $Ac + c = 0$ implies $c = 0$, and from $Bb + b = 0$ and $BAb + b = 0$ together we deduce $b = (\frac{m}{2}, 0, 0, 0, \frac{m}{2})$. Summarizing, we find the following table of space groups:

Table 3.5: Space groups in the pentagonal Bravais class

Point group	Gener.	Non-primitive translations	n	Ext. pattern
5	A		1	
$\overline{5}$	$\overline{A}$		1	
$5\,m$	A, B	$b = (\frac{m}{2}, \ldots, \frac{m}{2})$	2	m
$5\,2$	$A, \overline{B}$		1	
$\overline{5}\,m$	$\overline{A}, B$	$b = (\frac{m}{2}, \ldots, \frac{m}{2})$	2	m

The extinction pattern symbols are defined as in the previous paragraphs.

Chapter Four
Special Construction Methods

4.1 Introduction

In Chapter 1 we have described the general form of the projection method for the construction of quasiperiodic tilings. The question arises whether there are special choices of the acceptance region C which yield particularly simple tilings, composed of a minimal number of different tiles. Besides of simplicity, there are other criteria for the choice of C. In his celebrated papers, de Bruijn [dB1] described the Penrose patterns as the dual graph of a very simple grid. This grid approach can easily be generalized to other point group symmetries [GR, SSL] and is closely related to the projection method [dB1, GR]. For instance, Kramer and Neri [KN] used it for the construction of the threedimensional Penrose pattern with icosahedral symmetry. A problem of the original grid method was that the equivalent projection construction in general was based on a lattice with a rather high dimension, higher than the minimal dimension required by the point group symmetry. In general, using a non-minimal dimension leads to more complicated tilings. An exception is the Penrose pattern, which is based on a 5-dimensional cubic lattice, but nevertheless has a strikingly simple structure. The tenfold symmetry of the Penrose pattern would require only four dimensions. It is, however, possible to generalize this grid method so that it works with any lattice [KGR]. The price one has to pay is a rather complicated grid in general. There is a special case however, a tiling with twelvefold symmetry and particularly simple grid, which does not belong to the class considered in [GR, SSL]. The grid construction of this tiling has first been considered by Stampfli [St]. In the same paper [St], yet another construction method is described, which is based on a hierarchic procedure. We derive here the equivalent projection construction and prove thereby the quasiperiodicity of Stampfli's tilings.

4.2 The Classical Grid-Projection Method

Let $L \subset E^n$ be an n-dimensional lattice, and $\mathbf{e}_1, \ldots, \mathbf{e}_n$ a fixed lattice basis of L. We decompose E^n into two orthogonal subspaces, $E^n = E^{\parallel} \oplus E^{\perp}$, of dimensions d and $n-d$ respectively. We assume in the following that this decomposition is such that $E^{\parallel}$ contains no lattice vectors of L. As explained in chapter 1, we obtain quasiperiodic patterns by projecting the lattice points contained in a strip $S = C \times E^{\parallel}$ onto $E^{\parallel}$. Here we use a variant of this method: instead of projecting the vertices of the lattice contained in the strip S, we project the centers of the fundamental parallelohedra F spanned by the lattice basis $\mathbf{e}_1, \ldots, \mathbf{e}_n$ of L whenever these centers

are contained in the strip. Parallelohedra are the higher-dimensional analogs of parallelograms and parallelepipeds [Cox]. Henceforth, will use this expression for any dimension. This variation of the method does not change the class of structures which is obtained, for it can be compensated for by a suitable adjustment of the center of C. Furthermore, we make a special choice for C: C is a translation of the projection onto $E^\perp$ of one of these fundamental domains F spanned by the lattice basis under consideration. If E is the d-plane parallel to $E^\parallel$ passing through the center of C, then with this choice of C the center of a fundamental parallelohedron F is contained in S and therefore projected whenever F has non-zero intersection with E. The centers of the fundamental domains F form a lattice L^* isomorphic to L. With this choice of the cross section C of the strip, and with generic position of the center of C, there is a unique d-dimensional lattice hypersurface Σ of L^* contained in S. This lattice hypersurface consists of facets spanned by d-tuples of basis vectors of L. Since the vertices of the quasiperiodic tiling are the projections of the vertices of Σ, the tiling can be decomposed into finitely many different tiles, namely the projections of the d-facets of L^* contained in Σ. These tiles are all d-dimensional parallelohedra. Of course, there can be at most $\binom{n}{d}$ different tiles. If L has a non-trivial point symmetry leaving $E^\parallel$ invariant, many of these tiles may be congruent, differing only in their orientation.

The tiling constructed in the previous paragraph can be obtained also in a different way, namely as the dual of a grid. To see this we observe that the center of a fundamental parallelohedron F is projected whenever this parallelohedron has a non-zero intersection with E. The boundaries of all these parallelohedra are given by the union of n arrays of equidistant parallel $(n-1)$-dimensional lattice hyperplanes spanned by $(n-1)$-tupels of basis vectors of L. The intersection of all these hyperplanes with E, called the *grid*, is again a union of n arrays of equidistant parallel hyperplanes, this time of dimension $d-1$. The grid dissects E into open domains, called *meshes*, each of which corresponds to a parallelohedron F intersecting E. Therefore, with each mesh of the grid a vertex of the corresponding tiling is associated. If two meshes share a common $(d-1)$-face stemming from the j^{th} array of hyperplanes, then the associated lattice points are separated by $\mathbf{e}_j$, and so the positions of their projections relative to each other are determined. In this way we can construct the positions of all vertices from the grid alone. For generic position of E, at most d of the hyperplanes of the grid have a common intersection. With each intersection of d hyperplanes, a d-facet of the lattice L^* contained in Σ is associated. The vertices of this d-facet are the centers of the parallelohedra associated with the meshes which share the intersection point under consideration. Therefore, the dual graph of the grid is in fact the tiling constructed above by the projection method, i. e. the projection of the lattice hypersurface Σ.

In fact, the first global construction of the Penrose patterns used this grid approach [dB1], which was then generalized to other symmetries [B, KN]. Only later the projection approach became more popular [E1, DK], although it originates from de Bruijn's papers [dB1] too. A few examples are discussed in some detail in the next section.

4.3 The Penrose Pattern and Other Examples

In this section we would like to supply a few illustrating examples for the classical grid-projection method. Since we are interested in tilings with non-trivial, crystallographically forbidden symmetry in Fourier space, we have to start with a lattice which has a fundamental parallelohedron with this symmetry. Primitive orthogonal lattices always have a fundamental parallelohedron which has the full symmetry of the lattice, and since among the orthogonal lattices the cubic ones have the largest symmetry, our examples will be based on (primitive) cubic lattices.

The lowest dimension which allows for a crystallographically forbidden symmetry is four. The cubic group in four dimensions, consisting of all signed permutations of four elements (e. g. the four standard basis vectors), has a natural subgroup C_8. It therefore should be possible to construct an octagonally symmetric tiling from the four dimensionl primitive lattice with the grid-projection method. Indeed, we know the solution already from chapter 2. The octagonal lattice in four dimensions [Br], for the special choice of lattice parameters, $a_\parallel = a_\perp$, degenerates into a primitive cubic lattice. The invariant subspaces of the octagonal group we know already from chapter 2, and so the only new ingredient of the projection part of the grid-projection method is the acceptance region C. C is equal to the projection of a unit cube of the lattice onto $E^\perp$, which yields a regular octagon with edge-to-edge diameter $(1+\sqrt{2})a_\perp$. The tiling then can be obtained by projection as described in last section. It consists of the projections of 2-facets spanned by basis lattice vectors. Because of octagonal symmetry, only two different tiles occur (up to rotation), a square and a 45°-rhombus, both with edge length $a_\parallel$.

The grid associated with this tiling consists of the intersections with E of all lattice 3-planes spanned by three lattice basis vectors, which results in four arrays of equidistant parallel lines. The four unit normals of these arrays are parallel to the four projected basis vectors of L, $\mathbf{e}_1^\parallel, \ldots, \mathbf{e}_4^\parallel$. The tiling obtained by projection is the dual graph of this grid. An example of such an octagonal tiling is shown in Fig. 4.1. Octagonal tilings of this type have first been considered by Beenker [B].

In a similar way, icosahedral tilings can be obtained from a six-dimensional cubic lattice [KN, E1, DK]. The primitive icosahedral lattice degenerates for the lattice parameters $a_\parallel = a_\perp$ to a primitive cubic lattice. A unit cube projected onto $E^\perp$ yields the acceptance region, a rhombic triacontahedron. The tiling consists

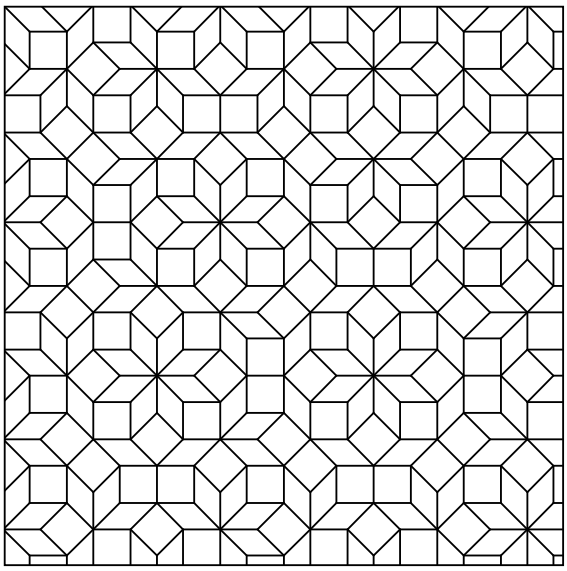

Fig. 4.1: An octagonal tiling

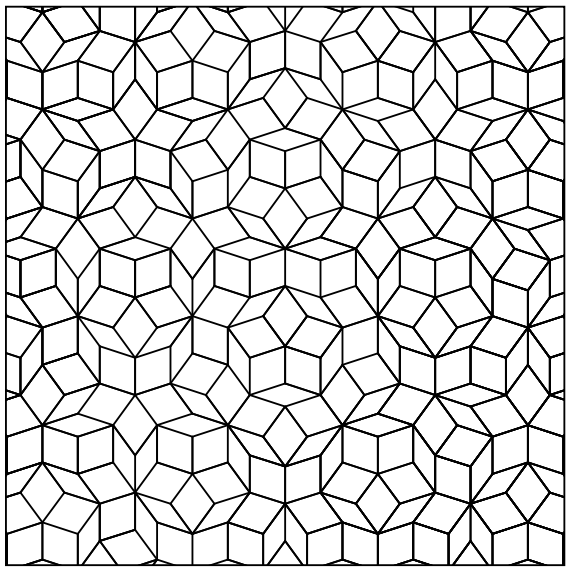

Fig. 4.2: A Penrose tiling

of projected 3-facets of L. Due to icosahedral symmetry, up to rotation only two different tiles occur (see e. g. [KN]). The grid of which this icosahedral tiling is the dual graph consists of six arrays of equidistant planes, the unit normals of which point to the vertices of an icosahedron.

The two examples above both have the property that $E^\perp$ doesn't contain any lattice vectors, i. e. we have used a lattice of minimal dimension. For the Penrose pattern this is not the case. The Penrose pattern is obtained from a five dimensional cubic lattice, which is a special case of the pentagonal lattice. However, the Penrose pattern is two dimensional, and so also the z-direction is projected, i. e. contained in $E^\perp$. The presence of lattice vectors in $E^\perp$ causes some problems. First, there are infinitely many local isomorphism classes, depending on the z-coordinate of the acceptance region in $E^\perp$. In our example, the acceptance region is the projection of a unit cube onto $E^\perp$, which yields a rhombic dodecahedron. The diameter in z-direction of this dodecahedron is equal to the length of the shortest lattice vector in z-direction. The projection onto $E^\perp$ of the lattice L is contained in an array of parallel equidistant planes perpendicular to the z-axis. There are five inequivalent types of these planes (see the discussion of the pentagonal lattice in chapter 2). Identical planes are five units apart. Therefore, the acceptance region generically cuts five of these planes. However, there is a discrete set of positions in z-direction for which the acceptance region fits exactly between two planes of the same type, intersecting only four of the others. This special position of the acceptance region leads to the Penrose pattern [KD]. The intersections of the rhombic dodecahedron with the four planes are two large pentagons, turned by 36° with respect to each other, and two smaller pentagons, also turned by 36° with respect to each other.

Each of the planes cuts the rhombic dodecahedron through the vertices with a fixed z-coordinate.

The projection method now can be applied as usual, yielding a tiling which consists of two types of rhombus, one with an acute angle of 36°, the other with 72° (Fig. 4.2). The grid consists of five arrays of equidistant, parallel lines, whose unit normals point to the vertices of a regular pentagon.

Although the rhombic dodecahedron has only five-fold symmetry, the Penrose pattern nevertheless has ten-fold symmetry, because the decoration of L with the acceptance regions is also inversion symmetric. Inversion symmetry maps one type of large (small) pentagon onto the other, and vice versa. Since an inversion resticted to a two dimensional subspace is a rotation by 180°, the Penrose pattern is indeed ten-fold symmetric.

The Penrose pattern has very special selfsimilarity properties. On the one hand, there is the scaling symmetry discussed in section 2.4. A Penrose pattern is mapped onto a subset of itself if we scale it by a factor of $-\tau^2$ with respect to one of those vertices which, when projected onto the plane perpendicular to the z-axis in $E^\perp$, fall into the intersection of the four pentagons discussed above. This intersection is a regular decagon. Besides of this scaling symmetry however, there are the famous inflation and deflation operations [dB1, Ga]. These are not of the type discribed in section 2.4. Inflation and deflation are based on the selfsimilarity mapping

$$M = \begin{pmatrix} 0 & 0 & 1 & 1 & 0 \\ 0 & 0 & 0 & 1 & 1 \\ 1 & 0 & 0 & 0 & 1 \\ 1 & 1 & 0 & 0 & 0 \\ 0 & 1 & 1 & 0 & 0 \end{pmatrix}. \tag{4.1}$$

Since $\det(M) = 2$, M maps L onto a subset of L. The space $E^\parallel$ is stretched by a factor $-\tau$, the representation space of the other two-dimensional irreducible representation of C_5 shrinks by a factor τ^{-1}, and the z-axis is stretched by a factor 2. This eigenvalue 2 makes it impossible that M maps the acceptance region onto a subset of itself. However, since two lattice points which differ only by a lattice vector parallel to the z-axis project onto the same point, in is sufficient that $M(C \cap L) \subset C \cap L$ modulo $(1, 1, 1, 1, 1)$. Since the small pentagons in the acceptance region are exactly by a factor of τ smaller than the large ones [dB1], this goal can be achieved [KD]. However, there is no freedom to choose the origin of this scaling – it is completely fixed by the position of C. In general, the origin of the scaling is not a lattice point, and so the new Penrose pattern is a subset of the old one, but not an enlarged copy of itself. The latter is the case only for the two exactly five-fold symmetric Penrose patterns.

4.4 The Generalized Grid-Projection Method

The main disadvantage of the grid-projection method described in section 4.2 is that for a general lattice there is no lattice basis spanning a parallelohedron which is invariant under the full point group of the lattice. This is the case only for orthogonal lattices. Even the projection of such a parallelohedron onto $E^\perp$ lacks the required symmetry in general. Therefore, if one wishes to construct a tiling with point symmetry G, one has to choose an orthogonal (or even cubic) lattice L of high enough dimension so that G can be embedded in the point group of L. For instance, for the Penrose pattern described in last section we had to use a 5-dimensional cubic lattice although the symmetry group of the Penrose pattern would require only dimension four. Since more dimensions make things more complicated in general, it would be desirable to have a grid-projection method which works with every lattice and produces tilings which are symmetric under the full point group of the lattice.

Such a procedure has been introduced in [KGR]. The main idea is to use, instead of a parallelohedron, a fundamental domain which reflects the full symmetry of the lattice. Recall that a fundamental domain of a lattice is a connected set $F \subset E^n$ which covers together with its lattice translates every point of E^n exactly once. Here, we choose a fundamental domain whose closure is the Voronoi domain of the lattice. The Voronoi domain associated with the lattice point $\mathbf{x}$ consists of all those points whose distance to $\mathbf{x}$ is not bigger than the distance to any other lattice point. Clearly, the Voronoi domain is invariant under the full point group of the lattice. In the rest of this section, we describe the general procedure. In the next section, we then illustrate it with an example.

The procedure is very simialar to that in section 4.2. Let $\mathcal{P}$ be the Voronoi cell packing or Voronoi partitioning of the lattice L. Voronoi cells in $\mathcal{P}$ will henceforth be called just "cells". Furthermore, let E a d-plane parallel to $E^\parallel$. We call the lattice point associated with a Voronoi domain $F \in \mathcal{P}$ the center of F. The vertices of the tiling to be constructed are the projections of those lattice points which are inside the strip $S = C \times E$, where C is the projection onto $E^\perp$ of the interior of a cell $F \in \mathcal{P}$ centered at E. This is equivalent to projecting the centers of all those cells $F \in \mathcal{P}$ which have a non-zero intersection with E.

Next, we have to divide E into tiles by specifying all their faces of dimensions up to $d-1$. The 1-dimensional "faces" are obtained by connecting all those vertices by a straight line whose associated cells share a common face of dimension $n-1$ which cuts E. If $d = 2$, the tiling is then completely specified. For $d > 2$ however, the situation is somewhat more complicated. Those lattice points whose associated cells share a face of dimension k are the corners of a convex polytope of dimension $n-k$. This can be seen as follows. The points whose cells share the k-face under

consideration can all be connected by a chain or net of straight lines each of which is perpendicular to an $(n-1)$-face containing the k-face and thus perpendicular to the k-face itself. Therefore, all these points are contained in a single plane of dimension $n-k$ perpendicular to the k-face. Hence, we can build the $(n-k)$-dimensional polytope dual to a given k-face. If now the k-face cuts E, we project its dual polytope to E. In this way we obtain a prescription for the subdivision of E into tiles. Note that with each projected dual of a k-face also all its boundaries are projected, since the k-face is contained in the corresponding $(k+1)$-faces which cut E too.

The same tiling can also be obtained as the dual of a grid G. This grid is given by the intersection of the union of the boundaries of all cells of $\mathcal{P}$ with the subspace E. The grid divides E into convex polyhedral cells, called *meshes*, the faces of which are the intersections of E with the $(n-1)$-dimensional faces of the cells of the partitioning. Each mesh of the grid corresponds to a cell which cuts E. Therefore, with each mesh we can associate the projection of the corresponding lattice point, and two lattice points belonging to meshes with a common $(d-1)$-face have to be connected by the projection of the corresponding lattice vector connecting the two lattice points. The vertices associated with the meshes sharing a common k-face will become the corners of a $(d-k)$-face of a tile (these vertices are indeed contained in a $(d-k)$-plane as explained in the previous paragraph). In this way we see that the tiling obtained previously by projection can be reconstructed from the grid. According to this construction, it is the dual graph of the grid.

What is not immediately clear is whether there will be overlapping tiles, i. e. whether the tiling is folded. Whether there are additional conditions required to avoid overlapping, and what these conditions would be, we leave as an open problem. We have some (numerical) evidence however that overlapping does not occur, and we conjecture that this generally true. For the classical grid method, the necessary and sufficient non-overlapping conditions have been determined [GR, dB2].

From the grid picture and from the periodicity of L it follows that the tiling consists only of a finite number of different tiles (up to translation), for there are only finitely many inequivalent $(n-d)$-faces of the cells of $\mathcal{P}$ which can cut E (note that the type of such an $(n-d)$-face determines which vertices belong to the associated cell). By a similar reasoning one finds that there are only finitely many arrangements of cells which share a common vertex, a result which has been obtained by more general arguments already in section 1.3.

4.5 Example: A Dodecagonal Structure

As an application of the generalized grid-projection method, we discuss the construction of a class of twodimensional tilings with twelvefold symmetric Fourier spectrum. These tilings have first been constructed by Stampfli [St] by means of a grid. More details about these and related tilings can be found in chapter 5.

The tilings we are going to study are based on the dodecagonal lattice L in four dimensions, as described in chapter 2. Recall that a generating star of twelve vectors, $\mathbf{e}_1, \ldots, \mathbf{e}_{12}$, is given by its projection onto $E^{\parallel}$ and $E^{\perp}$,

$$\begin{aligned} \mathbf{e}_i^{\parallel} &= a_{\parallel}(\cos(\pi i/6), \sin(\pi i/6)) \\ \mathbf{e}_i^{\perp} &= a_{\perp}(\cos(5\pi i/6), \sin(5\pi i/6)). \end{aligned} \tag{4.2}$$

The fundamental domain we will be using is the Voronoi domain. Hence we have to fix the ratio $a_{\parallel}/a_{\perp}$, for the geometry and even the topology of the Voronoi domain V of L sensitively depends on this ratio. The projection of V onto $E^{\perp}$ does not simply scale with $a_{\perp}$. A particularly simple Voronoi partitioning is obtained for $a_{\parallel} = a_{\perp}$, and therefore we will adopt this choice. For this choice of parameters, we obtain a maximally symmetric lattice in the diisohexagonal orthogonal primitive Bravais class [Br], which has a higher symmetry than the required dodecagonal one, of which we will not make use however.

Let us now construct the Voronoi partitioning of L. In chapter 2 we have seen that we can use $\mathbf{e}_1, \ldots, \mathbf{e}_4$ as a basis of L. Furthermore we note that the space spanned by $\mathbf{e}_1$ and $\mathbf{e}_3$, denoted by E^a, is orthogonal to the space E^b spanned by $\mathbf{e}_2$ and $\mathbf{e}_4$. The vectors $\mathbf{e}_1$ and $\mathbf{e}_3$ generate a regular 2d hexagonal lattice L^a in E^a, and $\mathbf{e}_2$ and $\mathbf{e}_4$ generate a corresponding lattice L^b in E^b. Therefore, L is given as an orthogonal sum of two 2-dimensional regular hexagonal lattices,

$$L = L^a \oplus L^b. \tag{4.3}$$

Next we recall the fact that in such a case the Voronoi domain of L is given by the product of the two Voronoi domains of L^a and L^b,

$$V = V^a \times V^b, \tag{4.4}$$

which of course are regular hexagons. Let H^a and H^b be the hexagons nets given by the boundaries of all Voronoi domains of L^a and L^b respectively. Then the union of the boundaries of all Voronoi domains of L is given by

$$N = (H^a \times E^b) \cup (E^a \times H^b), \tag{4.5}$$

i. e. N is the union of two orthogonal arrays of hexagonal "tubes". Let E be a generic plane parallel to $E^{\parallel}$. The *grid*, i. e. the intersection of N with E, is then the union

of the intersections of the two arrays of tubes, which are both regular hexagon nets, turned with respect to each other by 30° (see Fig. 4.3). The elementary hexagons of these nets are by a factor two larger than the projections of the Voronoi domains of the hexagonal lattices. The relative positions of the two nets are determined by the position of E.

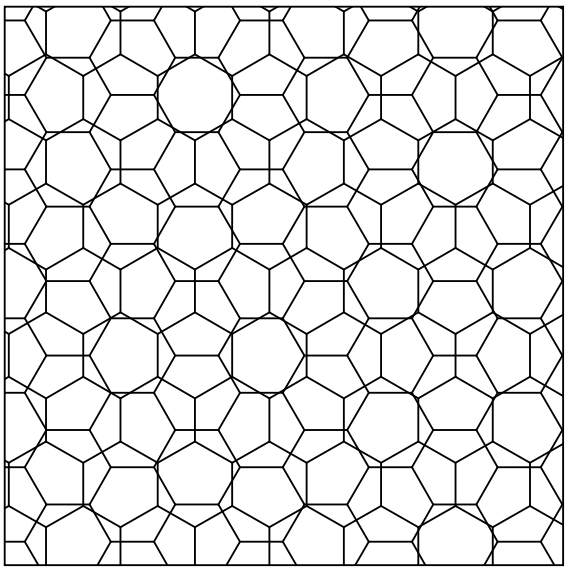

Fig. 4.3: Grid composed of two hexagon nets

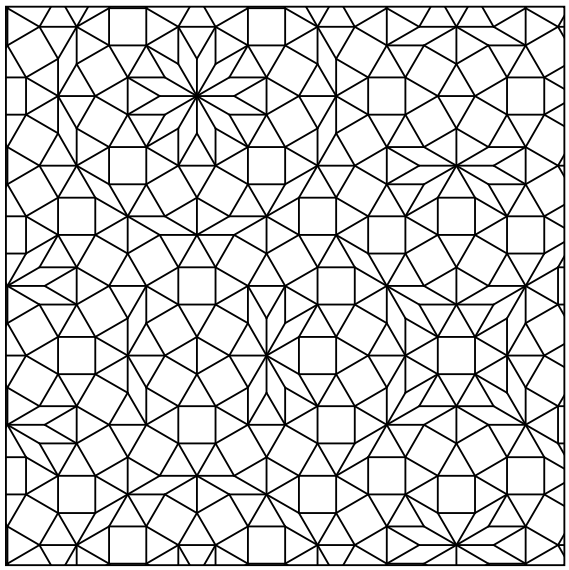

Fig. 4.4: Quasiperiodic tiling dual to grid of Fig. 4.3

For the construction of Stampfli's tilings, the two algorithms discussed in section 4.4 now read as follows:

A: *Projection construction*
Project the center of all those Voronoi domains of L onto $E^{\parallel}$ which cut E. Connect all those points by a straight line whose Voronoi domains have a face in common which cuts E.

B: *Grid construction*
With each mesh of the grid $N \cap E$, associate a vertex of the tiling. If the meshes of two vertices have a common face, these vertices are connected by a line of unit length which is perpendicular to this face. This is Stampfli's presciption.

A tiling constructed in this way is shown in Fig. 4.4.

Let us finally note that this is a particularly simple example, due to the fact that L is an orthogonal sum of two 2d lattices. From this it follows that the grid $N \cap E$ is the union of two simple periodic grids. In the general case, $N \cap E$ would be very complicated, but nevertheless all our constructions would go through as well.

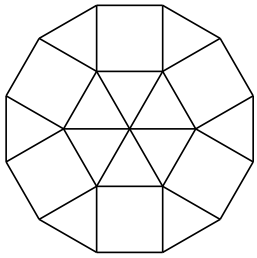
Fig. 4.5a

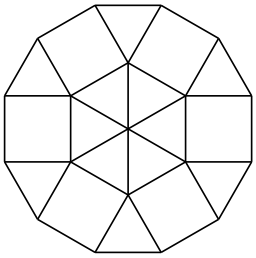
Fig. 4.5b

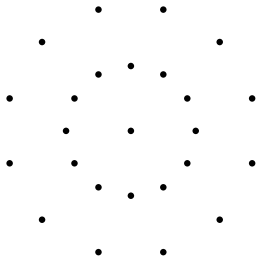
Fig. 4.5c

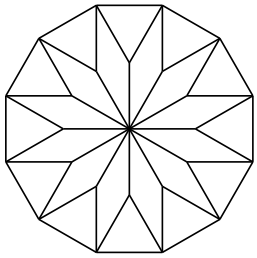
Fig. 4.5d

4.6 A Hierarchic Construction

In this section we explain Stampfli's hierachical construction [St] in terms of the projection method. Stampfli's method is briefly summarized as follows. We first choose a motif, e. g. a regular dodecagon, dissected into twelve equilateral triangles and six squares, as shown in Fig. 4.5a. We assume that the edges of the triangles and squares have unit length. This motif is the pattern of the first generation. To obtain the pattern of the $(n+1)^{th}$ generation, we take the vertices of the n^{th} generation pattern, scale this vertex distribution by a factor $2+\sqrt{3}$, replace each vertex by the motif, and draw the missing lines between all pairs of vertices with unit distance. The pattern of the second generation is shown in Fig. 4.6a. Patterns generated in this way have exact sixfold symmetry. The scaling factor $2+\sqrt{3}$ is chosen according to the following guide lines. The aim is to obtain a homogeneous, discrete distribution of vertices on the whole plane. Therefore, the scaling factor c may not be too large, for this would destroy homogeneity. On the other hand, since in each step each vertex is replaced by eighteen new vertices, while the area of the pattern grows only by a factor c^2, we must take care that we do not get a dense distribution of vertices. This can be achieved only if c is chosen such that vertices from different motifs coincide in certain cases, in order to reduce the growth of the effective number of vertices. This reasoning leads us to the choice $c=2+\sqrt{3}$, which is the edge-to-edge diameter of the dodecagon of Fig. 4.5a. Next we note that the inner hexagon of the motif could be replaced by one that is turned by 30°, as in Fig. 4.5b. In the iteration scheme, each vertex now can be replaced by a motif chosen randomly among the two possibilities. By introducing this randomness, we break the exact hexagonal symmetry. However, if we choose motifs with either orientation with the same probability, we can expect that the intensities in Fourier space have even twelvefold symmetry, even though we have may be no true δ-peaks any more (see below). A pattern with randomly oriented motifs is shown in Fig. 4.6b. It is evident that this hierarchic construction works as well with other choices of the motif, e. g. with motifs of different rotation symmetry. In each case, the scaling factor has to be chosen appropriately.

In order to connect this construction to the projection method, we first note that

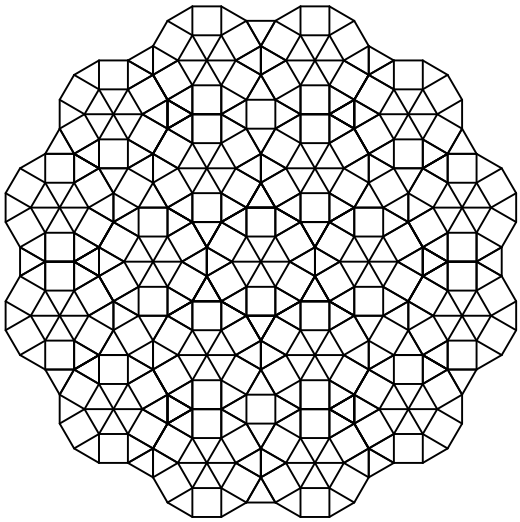

Fig. 4.6a

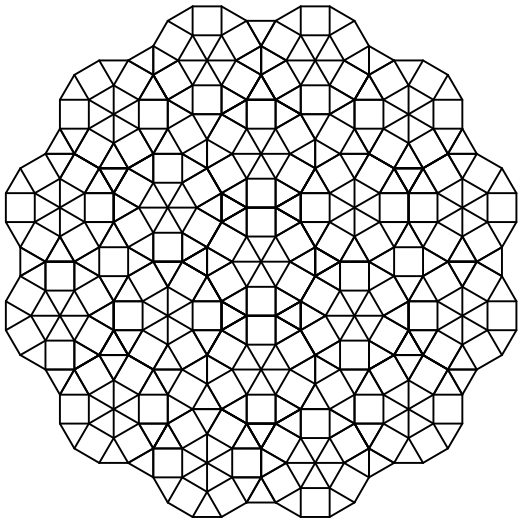

Fig. 4.6b

the scaling factor c is the same as in the selfsimilarity mapping discussed is chapter 2. This is no accident of course, as we will show now. It will be convenient to describe the iteration scheme in 4-dimensional space. The positions of the vertices can all be written as an integer linear combination of the vectors $\mathbf{e}_1, \ldots, \mathbf{e}_4$. Therefore, we can obtain the vertices of the pattern by projecting a unique set of "occupied" lattice sites of a dodecagonal lattice onto $E^{\parallel}$. Since the mapping M commutes with the projection onto $E^{\parallel}$, it can replace scaling by a factor $2 + \sqrt{3}$. First, we will explain the connection to the projection scheme by using a different motif, shown in Fig. 4.5c. This motif consists of the vertices of a twelvefold star of 30° rhombs (Fig. 4.5d). We do not draw the lines between the vertices because in the patters of higher generations this can't be done unambiguously. As compared to the old motif, we have replaced the vertices of the inner hexagon by those of a complete dodecagon. If we choose the parameters of the dodecagonal lattice L to be $a_{\parallel} = 1$, $a_{\perp} = \sqrt{2 + \sqrt{3}}$, then the motif is just the projection of the shortest 25 lattice vectors of L, the origin and 24 vectors with the same length. For these parameters, L is identical to the hypercubic Z-centered lattice [Br, Ras]. The Voronoi cell packing of this lattice is one of the regular honeycombs [Cox] in four dimensions, a packing of the famous 24-cell [Ras, Cox]. In this lattice, each site has 24 eqivalent neighboring sites.

The hierarchic construction is described as follows. The motif and pattern of the first generation is the projection of all vertices contained in a closed ball of radius $r = \sqrt{2 + \sqrt{3}}$ around the origin, or an open ball of radius $\sqrt{3}r$, or any ball of intermediate radius (all these balls contain the same set of vertices). Note that the projections of the contents of these balls onto $E^{\parallel}$ and $E^{\perp}$ are identical; what

in $\|$-projection is the inner dodecagon becomes in $\perp$-projection the outer one, and vice versa. Vertices inside the ball are said to be occupied. Now the iteration step is described as follows. First we apply M to the set of occupied sites. Then we add to the set of occupied sites all its nearest neighbors. Therefore, if S_n is the set of occupied sites of the n^{th} generation, S_{n+1} is given by the contents of the union of all r-balls centered at the vertices contained in MS_n. Clearly, since $\sum(2+\sqrt(3))^n < \infty$, S_n is contained in $C \times E^{\|}$, where C is some compact region $\subset E^{\perp}$. In order to see that there really exists an acceptance region $C \subset E^{\perp}$ such that $S_n \subset C \times E^{\|}$ for all n and that S_n fills $C \times E^{\|}$ completely as $n \to \infty$ we use a different but equivalent procedure. From above description one might think that S_n, as $n \to \infty$, fills a region which has a boundary which is "bumpy" even in $E^{\|}$-direction. That this is not the case can be seen as follows. Instead of applying M to S_n and then replacing each vertex in MS_n by the contents of an r-ball centered at this vertex, we could also replace each vertex of S_n by $M^{n-1}S_0$, which has exactly the same effect. But now the vertices of S_n are replaced by the contents of long and thin ellipsoids, from which it becomes evident that there really exists an appropriate acceptance region C. The set C is given by the limit of the strictly decreasing sequence of sets C_n defined as follows. Let B be a $\sqrt{3}r$-ball centered at the origin. C_1 is the projection of B onto $E^{\perp}$, and C_n, $n \geq 1$ is the projection of the union of ellipsoids M^nB centered at the vertices of S_{n-1}. For all n, C_n is connected and simply connected. This would not have been the case if we would have started with an r-ball B. Then C_n would have had holes, which would have been filled up asymptotically however. Avoiding this difficulty was the only reason to start with a larger ball.

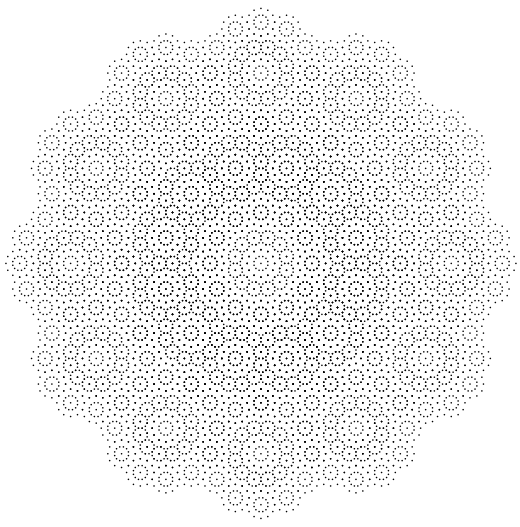

Fig. 4.6c

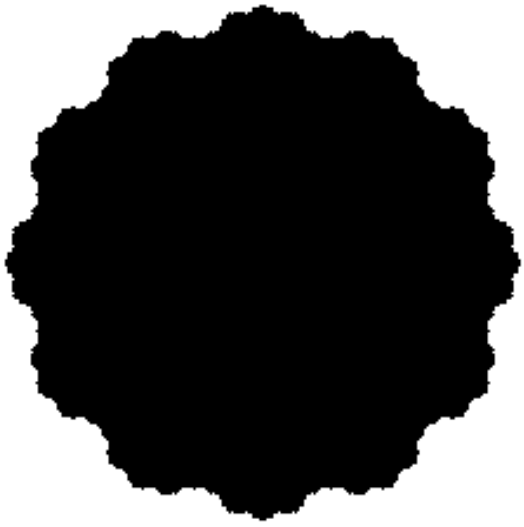

Fig. 4.7a

The pattern of the third generation corresponding to the motif of Fig. 4.5c is

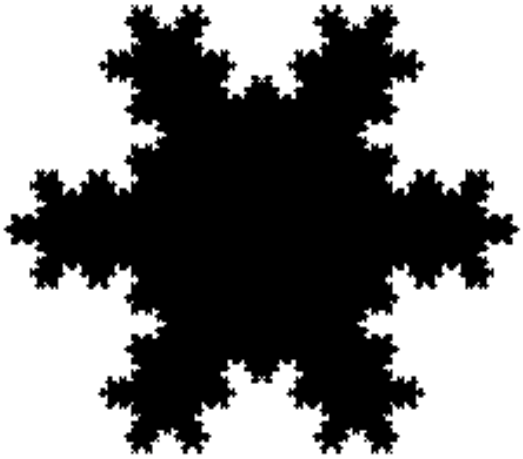

Fig. 4.7b

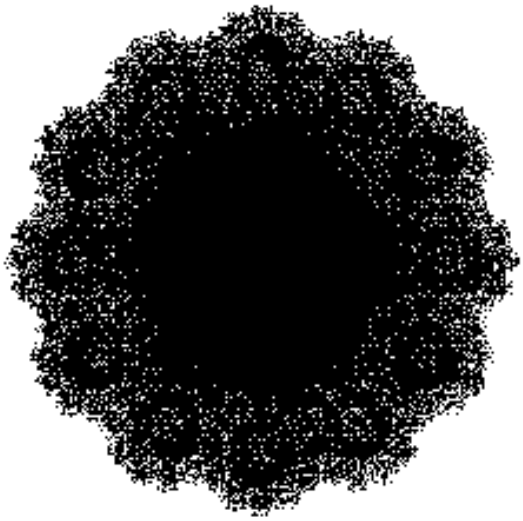

Fig. 4.7c

shown in Fig. 4.6c. The projection of the set S_3 onto $E^\perp$ looks exactly the same, but is on a different scale. Asymptotically, the projection of S_n onto $E^\perp$ fills C densely, and all points in $C \times E^\parallel$ are eventually projected. This is depicted in Fig. 4.7a. It is interesting to note that C has a fractal boundary. It can also be obtained by a van Koch type construction. One starts first with a dodecagon (including the interior) spanned by the motif, adds then smaller dodecagons centered at its corners, and so on. The fractal nature of the boundary of C should not have drastic effects on the diffraction pattern, and so it is not of much relevance physically.

Let us return to the motif of Fig. 4.5a. In this motif, six of the inner vertices are missing. If we project the corresponding lattice points onto $E^\perp$, six of the outer vertices are missing. Therefore, the sequence C_n now consists of sets which have roughly the shape of a hexagonal star. The limit of C_n is shown in Fig. 4.7b. We see that the boundary of this set apparently has a fractal dimension which is larger than that of Fig. 4.7a. The starting set of the corresponding van Koch construction would in this case be a hexagonal star. In the iteration, at each corner one has to add a smaller star, and so on.

We would like to emphasize that although this pattern has only hexagonal symmetry, its diffraction pattern nevertheless requires a dodecagonal indexing. The dodecagonal symmetry of the underlying lattice has been broken only by the decoration. The intensities of the diffraction pattern will show hexagonal symmetry, whereas the set of all peak positions will be twelvefold symmetric.

Up to now, we have considered patterns which have exact twelve- or sixfold symmetry. These patterns can be obtained by the projection method and are therefore quasiperiodic. If we choose randomly among the two orientations of the motif

of Fig. 4.5a, this is not the case any more. These "random" patterns are obtained by projecting sets S_n which are defined as follows. S_1 is as for the hexagonal patterns; S_{n+1} is then obtained from S_n by replacing each point of MS_n randomly by the motif correspondig to one or the other orientation. Note that it is not equivalent any more to replace each vertex of S_n by a scaled motif — this would introduce unnatural long range correlations between the orientations of the inner hexagons. The acceptance region corresponding to this random pattern is an average of two hexagonal regions as in Fig. 4.7b, turned with respect to each other by 30°. Those points whose $\perp$-projection falls into the intersection of the two hexagonal stars are all projected onto $E^{\parallel}$, those whose $\perp$-projection falls only into *one* of the hexagonal stars may be projected or not, depending on to which motif orientation this point belongs. Therefore, the acceptance region has a deterministic core, and a "fuzzy" shell. This is shown in Fig. 4.7c. Although the probability that a point falling into the fuzzy region is projected onto $E^{\parallel}$ is certainly not independent of what happens to other points, it is may be a valid approximation to project those points just with a certain a priori probability. This would then produce diffraction patterns with true δ-peaks and twelvefold symmetric intensity distribution. As far as the true random patterns are concerned, without the approximation of independent probabilities, probably the δ-peaks have to be replaced by peaks with a finite width, but we do not expect a breaking of twelvefold symmetry.

We have illustrated this hierarchic construction with an example of (effective) twelvefold symmetry, but it is apparent that the same method works also with motifs of any other symmetry. The example discussed above is however the only one we have found which yields a tiling with such a simple structure, with just three different tiles.

Chapter Five
The Structure of Dodecagonal Quasicrystals

5.1 Introduction

In this chapter we present a detailed model structure for dodecagonal quasicrystals [INF1, INF2, CLK]. Most of the material in this chapter has been presented also in [G2]. Up to now, model structures have been presented for two types of icosahedral quasicrystals, i-$AlSiMn$ and i-(Al, Zn)-Mg [EH, HE]. Both of these are closely related to existing periodic phases, the key idea being to keep as much of the local configurations of the periodic phases as possible. This is a useful strategy also in the dodecagonal case. The dodecagonal phase of Ni-Cr [INF1, INF2] always occurs together with the σ-phase [BS] of the same material, and a comparison of high resolution electron micrographs (HREMs) of the two phases suggests that they are closely related. The HREMs of both phases show bright spots. If we connect these bright spots by straight lines, we obtain tilings composed of squares and equilateral triangles and, in the dodecagonal phase, of a few 30° rhombs. In the case of the σ-phase it is known that these squares and triangles, which form a semiregular tesselation with Schläfli symbol [Cox] $(3^2 \cdot 4 \cdot 3 \cdot 4)$, correspond to certain building blocks of the σ-phase. These building blocks, prisms with square or triangular base, form layers as the HREMs indicate. The layers are stacked periodically. Therefore, it is natural to assume that the dodecagonal phase is composed of the same building blocks, except that the arrangement within a layer is quasiperiodic instead of periodic. Moreover, another type of building block occurs in the dodecagonal phase, a prism with a 30°-rhombus as base. Since this third building block is rather thin, its atomic decoration can be completely derived from that of the surrounding blocks.

In the remaining sections, we first construct a quasiperiodic tiling which is very similar to the HREMs of the dodecagonal phase. It is therefore a good candidate for a decoration with the building blocks of the σ-phase. These building blocks are then described, so that a complete description of the model structure is provided. We then construct a five dimensional periodic structure such that the quasiperiodic model structure is the restriction of the periodic structure to a suitably embedded three dimensional subspace (physical space). The construction of the 5d periodic structure makes manifest that it has a non-symmorphic space group, containing a screw axis and a set of glide planes. After the determination of the frequency module (or reciprocal lattice) and the systematic extinction rules associated with

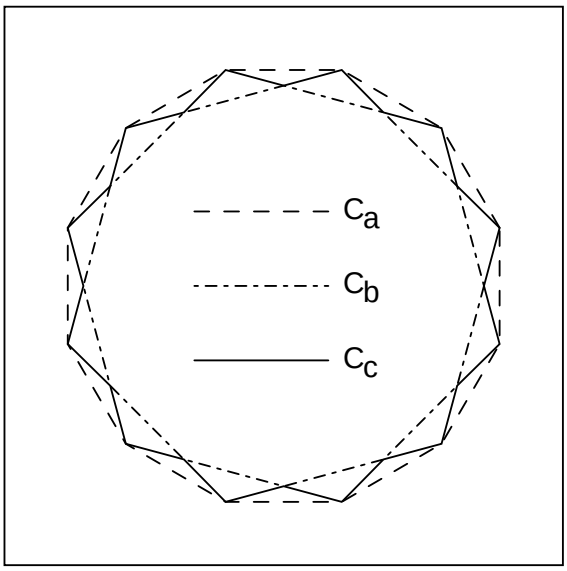

Fig. 5.1 Different acceptance regions

the space group, we calculate the electron diffraction patterns. This calculation includes multiple scattering effects, which are essential for electron diffraction. The calculated diffraction patterns compare well with the experimentally observed ones, as far as available. The systematic extinctions predicted by the space group analysis are present also in the calculated patterns. Unfortunately, the corresponding experimental patterns are still missing. However, decagonal [Be, F] quasicrystals show very similar extinction patterns, so that the occurrence of non-symmorphic space groups for quasicrystals is well established.

5.2 The Dodecagonal Tiling

In this section we construct a quasiperiodic tiling suitable for decoration with the basic building blocks of the σ-phase. Our starting point is the tiling of Fig. 4.3, which is obtained by the projection method with acceptance region C_a, a regular dodecagon (Fig. 5.1). When compared with high resolution electron micrographs [INF1, INF2, CLK], this pattern shows too many thin rhombs. Therefore, we have to eliminate some of the vertices by choosing a smaller acceptance region C_b. If we want to avoid nearest neighbor distances as small as the short diagonal of a thin rhombus, we have to take care that the corresponding lattice vector projected onto $E^\perp$ does not fit into C_b. The largest such acceptance region is again a regular dodecagon, but now turned by 15°, and with edge-to-edge diameter $2\cos(\pi/12)$ (see Fig. 5.1). The tiling obtained with this smaller acceptance region is shown in Fig. 5.2, from where one can see that a new tiling unit has been introduced. Therefore, it might be wise to eliminate only part of the thin rhombs, such that the remaining ones are isolated, sharing at most one vertex with each other. For this

purpose we have to choose C as large as possible but such that the projections of the origin, $\mathbf{e}_1$, $\mathbf{e}_2$ and $\mathbf{e}_3$ (or a symmetry equivalent set) do not fit simultaneously into C. This can be accomodated by choosing a non-convex acceptance region C_c as shown in Fig. 5.1. It is given by the union of two regular hexagons, turned with respect to each other by 30°. Note that C_b is the intersection of these two hexagons, while C_a is the convex hull of C_c. This last tiling, shown in Fig. 5.3, seems to be well suited to describe dodecagonal quasicrystals, for it looks very similar to the high resolution electron micrographs [INF1, INF2, CLK]. The tilings of Figs. 5.2 and 5.3 have independently been obtained also by Niizeki and Mitani [NM].

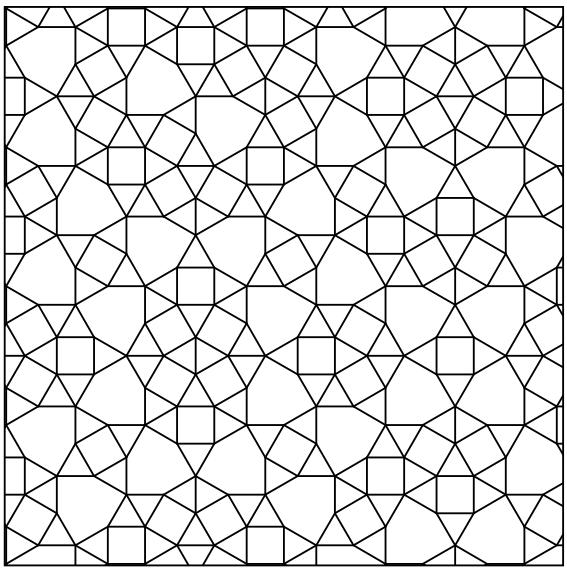

Fig. 5.2 Pattern based on C_b

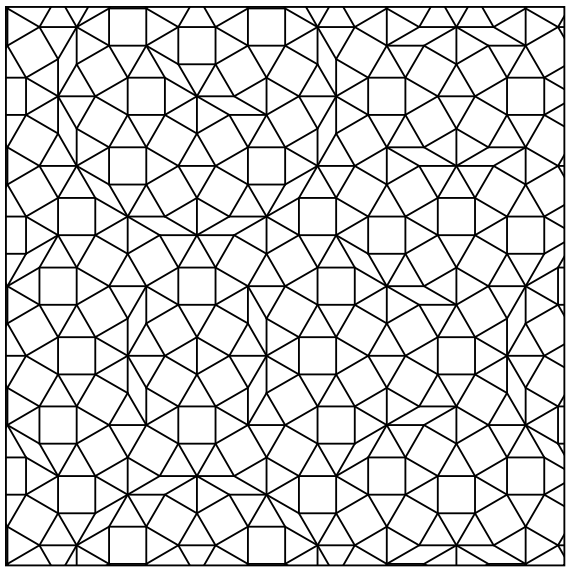

Fig. 5.3 Pattern based on C_c

The similarity of the tilings of Fig. 5.3 with the HREMs can still be improved by introducing disorder. Tiling 5.3 contains too many rhombs, but instead lacks regular hexagons composed of six equilateral triangles. These latter configurations occur relatively frequently in the HREMs. These deficiencies can be cured by locally rearranging some of the tiles. This is known as Hendricks-Teller disorder [HT, DV] and occurs very frequently in quasicrystals. It is even allowable to replace two thin rhombs by a square — not only the area is preserved in this process, but also the number of atoms (see next section). For instance, we could replace the contents of the dodecagon of Fig. 5.4 by that of Fig. 5.5.

The occurrence of disorder in dodecagonal quasicrystals is very natural. Although quasicrystalline *Ni-Cr* is produced by a different technique [INF1, INF2] than other quasicrystals, it still is obtained by a rapid quenching process. Since structural units corresponding to a thin rhomb occur in equilibrium phases only in the form of defects (in the σ-phase of *Fe-Cr* [I, IKM]), we expect that the alloy tries to avoid these rhombs, but does not quite succeed. During the rapid freezing,

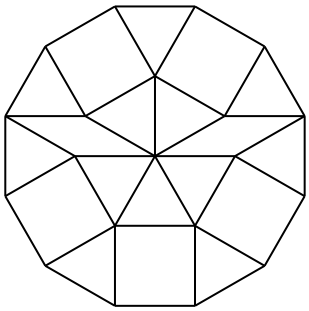

Fig. 5.4

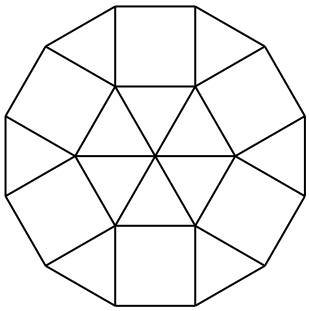

Fig. 5.5

the rigid and stable structural units corresponding to squares and triangles form at different places and with different orientations and then have to pack together somehow. Often this is possible only by introducing a thin rhomb. We believe that by this process effective twelvefold symmetry and quasiperiodicity is introduced, at least over a length scale corresponding to the size of the specimen (a few 100Å). Over these length scales, it should then be possible to describe such a structure by a disordered version of a truely quasiperiodic tiling. Even if there is a stable or metastable "ideal" phase which is truely quasiperiodic, by the rapid quenching process we would expect a considerable amount of disorder.

Disorder in quasicrystals has been discussed by various authors (see e. g. [DV, Ho, SLS]). The main idea has been to assume an acceptance region whose position in $E^\perp$ fluctuates. This results in the projection of the contents of a wavy strip. Elser [E2, E3] argued that the characteristic function of the acceptance region C could then be replaced by a smooth function, e. g. a gaussian, such that we obtain an effective acceptance function which accepts vertices only with a certain probability. In this approximation the diffraction pattern would still consist of sharp δ-peaks. Such a wavy strip produces local reorderings of some tiles, which is precisely the type of disorder we need. Defects corrsponding to such disorder are called phasons [SLS, Lu, BH]. For icosahedral quasicrystals the effects of such phasons can be observed experimentally (see e. g. [SLS, Lu, BH]), and also in the dodecagonal case there are hints for the existence of phason strains [INF2].

5.3 The Atomic Decoration

As we have seen earlier, the HREMs suggest a decoration of the squares and triangles of the dodecagonal tilings by the corresponding structural units of the σ-phase. These units are shown in Fig. 5.6, along with the decoration of the thin rhomb. For isolated thin rhombs the decoration shown in Fig. 5.6 is enforced by their surrounding. This decoration has been proposed by Ishimasa et al. [INF1]. From Fig. 5.6 we see that the layers at $z = 1/4, z = 3/4$ contain atoms at the vertices of the dodecagonal tiling, whereas the layers at $z = 0$ and $z = 1/2$ consist of atoms

placed on the midpoints of some bonds, along with possibly some atoms in the interior of the squares and triangles, depending on the orientation of these figures (see Fig. 5.6). In the $z = 0$ layer, only bonds parallel to $\mathbf{e}_i^{\parallel}$ with i even are occupied, whereas in the $z = 1/2$ layer those with i odd are occupied, so that the decoration of the latter two layers breaks the dodecagonal symmetry of the underlying pattern to a hexagonal one. Therefore, if we denote the $z = 1/4$ (or $z = 3/4$) layer by A, the $z = 0$ layer by B and the $z = 1/2$ layer by C, the structure is given by a stacking $\ldots ABAC \ldots$, where the layers A have dodecagonal symmetry, whereas the layers B and C have hexagonal symmetry.

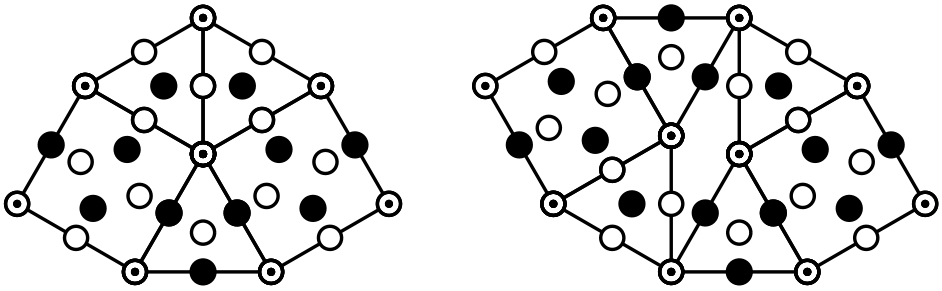

Fig. 5.6. The basic building blocks. Shown are a typical configuration for the σ-phase (left) and a typical configuration involving the 30°-rhomb (right). Full circles denote atoms at z=0, open circles atoms at z=$\frac{1}{2}$, and dotted circles atoms at z=$\frac{1}{4}$ and z=$\frac{3}{4}$.

A similar structure for dodecagonal quasicristals has been proposed by Yang and Wei [YW]. Their structure can be understood as an alternating stacking of a layer D and its mirror image $\tilde{D}$ (where the mirror is plane perpendicular to the z-axis). The layer D is essentially a decoration of the vertices of the tiling of Fig. 5.2 by slightly distorted hexagonal antiprisms containing an additional atom at their center. Because of the great similarity of this structure to ours, the diffraction pattern is expected to be very similar too. Nevertheless we consider our decoration as preferable, for the following reason. As we have argued above, the bright spots in the HREMs can be identified with those columns of atoms containig the atoms of the layers A. These columns are doubly occupied as compared to those containing the atoms of the layers B or C. In these HREMs most of the symmetric hexagons, as they occur in Fig. 5.2, contain an additional bright spot in their interior, which suggests a dissection of these hexagons into a square, two equilateral triangles and a thin rhomb. Therefore, our decoration, which breaks the threefold symmetry of these hexagons, seems more appropriate than that of Yang and Wei [YW].

5.4 The 5d Periodic Structure

Despite of the presence of the hexagonal layers B and C the structure has point group 12/mmm and therefore twelvefold symmetric Fourier spectrum. Since the main axis of the hexagonal layers are turned with respect to each other by 30°, the stacking sequence suggests a 12_6-screw axis. Moreover, the mirror B (3.6) maps the main axis of the layer B onto those of the layer C, and vice versa, so that we can expect as well that the mirror B is actually a glide mirror, translating the structure by half a period length into z-direction.

To make these intuitive arguments about the space group more rigorous, we construct a 5d periodic structure with this space group such that the quasiperiodic structure described above is the restriction of this periodic structure to a suitably embedded 3d subspace.

As explained in chapter one, it is useful to reformulate the projection method. Instead of projecting all vertices in the strip $L \cap (C \times E)$ onto $E^{\parallel}$ and then decorating them with the scattering density $\rho(\mathbf{x}_{\parallel})$ of an atom or cluster of atoms, we can as well decorate each vertex of L with a density $\rho(\mathbf{x}_{\parallel}) \cdot \chi_{\bar{C}}(\mathbf{x}_{\perp})$ (where $\bar{C}$ is the set C inverted at the origin, and $\chi_{\bar{C}}(\mathbf{x}_{\perp})$ the characteristic function of $\bar{C}$) and then take the intersection of the so obtained periodic density with E, which yields the same result. This latter formulation, first used by Janssen [J1] and Bak [Ba], is much more flexible than the original projection method. In particular, it is easy to add more atoms of various types at different positions in the unit cell of L, each with its own characteristic acceptance region. In this way also very complicated quasicrystals (including atomic decoration) can be viewed as the restriction of a higher-dimensional periodic structure to physical space. Since the Fourier spectrum of such an restriction is just the projection of the Fourier spectrum of the higher-dimensional periodic structure to physical space, classical crystallography can be applied to the periodic structure to determine the Bravais class, point symmetry and space group associated with a quasicrystal. The quasicrystal inherits in this way the point symmetry and the characteristic extinctions associated with the higher-dimensional space group. Therefore, we can speak of the space group of a quasicrystal, which we define to be that of the associated higher-dimensional periodic structure.

Next we construct the 5d periodic structure. In chapter two we saw that there is a unique dodecagonal lattice L^5 in five dimensions. This lattice is a stacking of 4d lattices L, $L^5 = L \times a_z Z$, where a_z is the periodicity in z-direction. This lattice is contained in a 5d space $E^{\parallel} \oplus E^{\perp} \oplus E_z$. We will use the lattice basis (2.4). $\mathbf{e}_5 \equiv \mathbf{e}_z$ is the basis vector in z-direction, which is the periodic direction of the quasicrystal. Sometimes, it is convenient to use the compound notation $(\mathbf{x}, z)$, where the first item denotes the first four coordinates in $E^{\parallel} \oplus E^{\perp}$. We construct the periodic structure in such a way that it becomes manifestly invariant under the space group generated

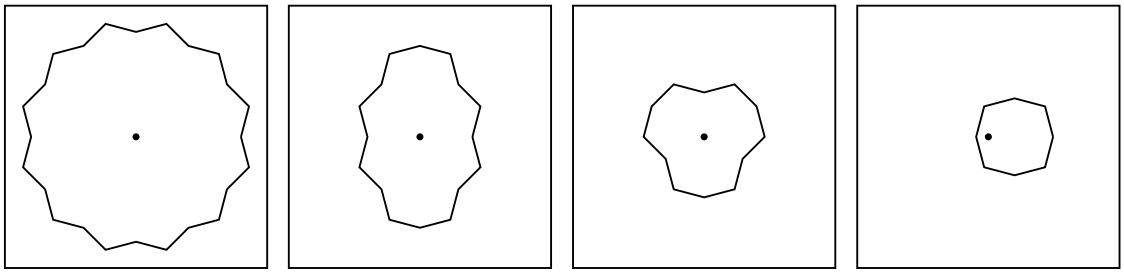

Fig. 5.7: Acceptance regions for atoms on a vertex, on a bond, in a triangle and in a square (from left to right).

by (A, a), (B, b), $(-I, 0)$ and the set of lattice translations. Here, A and B are the generators (3.6), (X, x) denotes the Euclidean transformation $y \to Xy + x$, and $a = b = (0, 0, 0, 0, \frac{1}{2})$.

First we place an atom with acceptance region C_a (see Fig. 5.7) at $(\mathbf{v}, \frac{1}{4})$, where $\mathbf{v}$ is a lattice site of L. Then we act with all the desired symmetry elements on this motif. The lattice translations put an atom at all sites in $L^5 + (0, \frac{1}{4})$. Moreover, for each atom at $(\mathbf{v}, z)$ the screw axis puts another copy at $(\mathbf{v}, z + \frac{1}{2})$. Since the acceptance region has dodecagonal symmetry, it is not changed under this screw operation. The other symmetry elements leave the structure obtained so far invariant. Note that the acceptance region is invariant also under the mirror B. Next we insert the atoms on the bonds of the tiling. We put an atom on the midpoint of a bond of L which is parallel to $\mathbf{e}_2$, at $z = 0$. The acceptance region is chosen in such a way that it intersects physical space $E \times E_z$ if and only if the acceptance regions of the two atoms at the vertices at the ends of this bond intersect $E \times E_z$ too. This results in an asymmetric acceptance region shown in Fig 5.7. Then we add all translation equivalent atoms. Appling the screw operation puts atoms on all the other bonds, those on bonds parallel to $\mathbf{e}_i$ with i even at $z = 0$, the remaining ones at $z = \frac{1}{2}$. Due to the rotational part of the screw operation, the acceptance regions of all these atoms will have their proper orientation. Again, the glide mirror (B, b) leaves the structure obtained so far invariant. Analogously, we put an atom in the middle of a triangle in the lattice L which projects to a triangle of the tiling, at $z = 0$ or $z = \frac{1}{2}$ (depending on the orientation of the triangle), and with acceptance region shown in Fig. 5.7. This acceptance region intersects physical space if and only if those at the corners of the triangle do so too. Acting then with the space group on this atom puts copies to the interiors of all triangles at the correct z coordinate, depending on the orientation of these triangles. Finally, we put an atom into the interior of a square in the lattice L. This time, we have to use an acceptance region which is not centro-symmetric (Fig 5.7), because the four corners of the square, whose acceptance regions have to cut physical space too, are at different distances. Acting then with the space group on this atom completes the structure. Note that

the space group takes care that all atoms have their correct z-value, and that their acceptance regions have the proper orientation. Therefore, the 5d periodic structure is manifestly invariant under a non-symmorphic space group, and the quasicrystal structure is the restriction of this periodic structure to physical space $E \times E_z$.

5.5 The Reciprocal Lattice and Extinction Rules

First, we calculate the reciprocal lattice $\hat{L}^5$ of L^5. Since L^5 is a periodic stacking of L, $\hat{L}^5$ is given by $\hat{L} \oplus (2\pi/a_z)Z$, so that is sufficient to calculate the reciprocal lattice $\hat{L}$ of L. It is convenient to choose $a_\perp = a_\parallel$, but any other choice of $a_\perp$ would give the same result. The metric tensor of L, defined by $g_{ij} = \mathbf{e}_i \cdot \mathbf{e}_j$, is given by

$$g = a_\parallel^2 \begin{pmatrix} 2 & 0 & 1 & 0 \\ 0 & 2 & 0 & 1 \\ 1 & 0 & 2 & 0 \\ 0 & 1 & 0 & 2 \end{pmatrix}. \tag{5.1}$$

Let $\{\mathbf{b}_i\}$ be the basis reciprocal to $\{\mathbf{e}_i\}$, i. e. $\mathbf{b}_i \cdot \mathbf{e}_j = 2\pi\delta_{ij}$. Then, if the i^{th} row of the matrix b contains the components of $\mathbf{b}_i$ with respect to the basis $\{\mathbf{e}_i\}$, we have

$$(bg)_{ij} = \sum_k b_{ik}\mathbf{e}_k \cdot \mathbf{e}_j = \mathbf{b}_i \cdot \mathbf{e}_j = 2\pi\delta_{ij}, \tag{5.2}$$

i. e. b is equal to 2π times the matrix inverse of g, which is given by

$$g^{-1} = \frac{1}{3a_\parallel^2} \begin{pmatrix} 2 & 0 & -1 & 0 \\ 0 & 2 & 0 & -1 \\ -1 & 0 & 2 & 0 \\ 0 & -1 & 0 & 2 \end{pmatrix}. \tag{5.3}$$

Comparison with (2.4) shows that $\hat{L}$ is again a dodecagonal lattice, but this time with lattice parameters

$$\hat{a}_\parallel = \frac{2\pi}{3a_\parallel^2} \cdot a_\parallel\sqrt{3} = \frac{2\pi}{a_\parallel\sqrt{3}}, \quad \hat{a}_\perp = \frac{2\pi}{a_\perp\sqrt{3}}. \tag{5.4}$$

Therefore, the peak positions in the quasiperiodic plane are generated by a twelvefold symmetric star of vectors $\mathbf{b}_i^\parallel$ which have length $\hat{a}_\parallel = 2\pi/a_\parallel\sqrt{3}$.

Let us now turn to the extinctions in the Fourier spectrum caused by the space group. Recall that (chapter 3, p. 32) a peak k is extinct whenever there exists a space group element (X, x) such that

$$e^{ik\cdot x} \neq 1 \quad \text{and} \quad \hat{\rho}(k) = \hat{\rho}(X^{-1}k). \tag{5.5}$$

In the present case this means that due to the screw symmetry of dodecagonal quasicrystals we can expect that all peaks $(0, k_z)$ are extinct whenever k_z is odd.

Similarly, the glide mirror symmetry causes all peaks k contained in a glide plane and with k_z odd to be absent. These extinctions can be understood also intuitively. The point is that at least in kinematical theory scattering with a scattering vector k is sensitive only to the projection of the structure onto this scattering vector. But since the projection of the layers B and C onto the z-axis give the same density, a scattering vector parallel to the z-axis sees a structure with half the period length, and therefore every second peak is absent. Similarly one can argue for the glide mirror plane, though the situation is slightly more complicated there.

One should note however that multiple diffraction, which occurs always with electron diffraction, might distroy this effect. Nevertheless, such extinctions are very typical for quasicrystals which are periodic in one direction. They have been observed already for decagonal [Be, F] quasicrystals. Our numeric calculations (see next chapter), which include multiple scattering, show that these extinctions have to be expected also in the dodecagonal case.

5.6 Calculation of the Diffraction Pattern

Since we have described our quasicrystal structure by means of a 5d periodic structure, it is now easy to compute its Fourier spectrum. We simply have to calculate the Fourier transform of the periodic structure and then project it onto physical reciprocal space. The Fourier transform of a periodic structure is obtained by first calculating the Fourier transform of the contents of a unit cell and then convoluting it with the reciprocal lattice, just as one does it with 3d crystals. The $z = 0$ layer of the Fourier transform of the quasicrystal is shown in Fig. 5.8. The radius of the circles is proportional to the *amplitude* (not intensity) of a peak. We see that Fig. 5.8 consists essentially of a single ring of very strong spots, the next weaker ones being more than ten times weaker (in intensity). This is very different from what one sees in electron diffraction [INF1, INF2, CLK], and also different from what one obtaines if one puts just atoms at the vertices of the tiling [NM], which would actually give a very good fit with experiment. The additional hexagonal layers lead to destructive interferences, so that only a few very prominent peaks survive.

We have to recall however that electrons are very strongly scattered by the coulomb potential, so that we have to take into account multiple scattering effects. This can be done by Darwin's method [Hi]. In electron diffraction, the incoming k-vector is much larger than the relevant scattering vectors, so that all scattering vectors which contribute to elastic scattering are contained essentially in a tangent plane of Ewald's sphere, i. e. only scattering vectors contribute which are contained in a plane through the origin and perpendicular to the incoming k-vector. All scattered beams can be indexed by the reciprocal vectors in this plane. Let ϕ_q

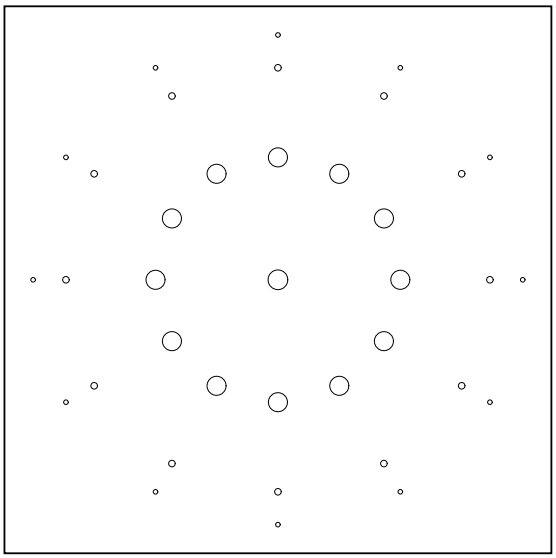

Fig. 5.8: The Fourier transform

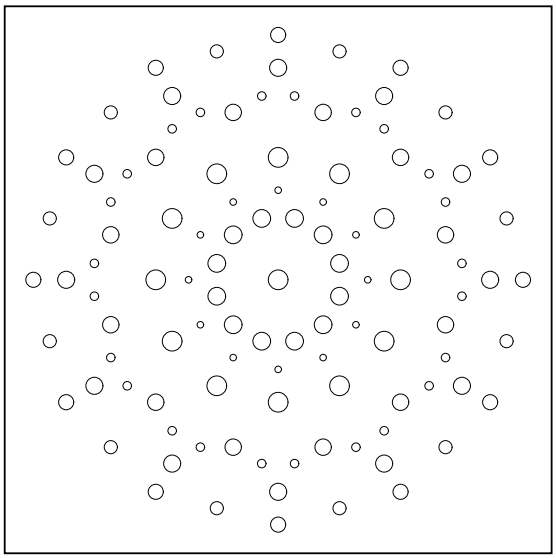

Fig. 5.9: Dodecagonal plane

denote the amplitude of such a scattered beam, and f_q the amplitude of the Fourier transform. While the beams pass through the quasicrystal, their amplitudes develop according to

$$\frac{d\phi_k}{dz} = \lambda i \sum_q \phi_{k-q} f_q, \tag{5.6}$$

where z measures the depth in the quasicrystal in the incoming beam direction, and λ is a constant depending on the density and type of atoms in the material. The sum extends over all reciprocal vectors in the plane perpendicular to the incoming beam, and the factor i in front of the sum ensures that the total intensity remains constant. In fact, it is easy to show that

$$\frac{d}{dz} \sum_q \phi_q \phi_q^* = 0. \tag{5.7}$$

Starting with $\phi_0 = 1$, $\phi_q = 0$ $(q \neq 0)$ equation (5.6) can easily be integrated numerically. We have chosen the integration domain such that we obtain best possible coincidence with the experimentally observed patterns. The step width in the numerical integration was determined such that about 40 iterations were necessary. In the dodecagonal plane, 3721 scattering vectors were included, whereas in the planes containing the z-axis 729 vectors were sufficient. The results are shown in Fig. 5.9 (dodecagonal plane) and Figs. 5.10 and 5.11 (mirror plane* and glide mirror plane respectively). Again, the radii of the circles are proportional to the amplitudes.

*the planes between two neighboring glide planes are true mirror planes

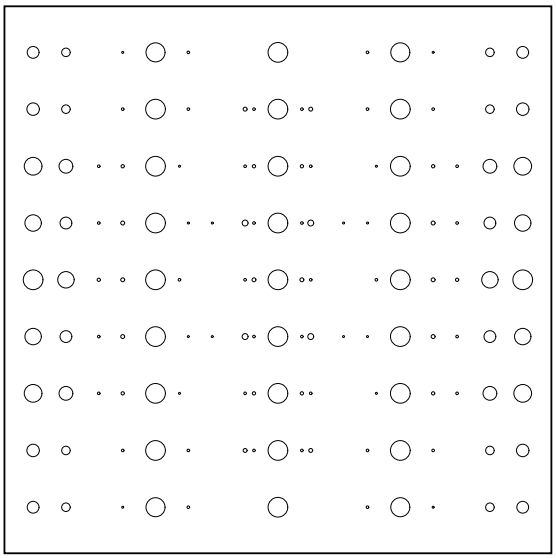

Fig. 5.10: Mirror plane

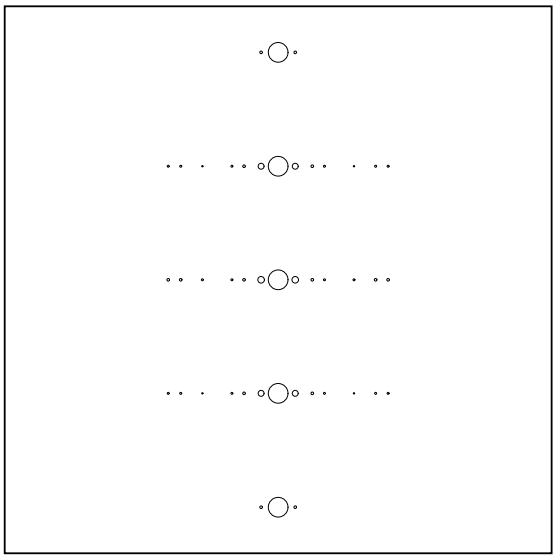

Fig. 5.11: Glide plane

All these calculated diffraction patterns compare very well to the observed ones, as far as available [INF1, INF2, CLK]. If we compare Figs. 5.8 and 5.9 we see that due to multiple scattering many additional peaks have appeared, in particular two additional rings very close to the center. This is very similar to what happens in the σ-phase of Fe-Cr. The σ-phase has peaks very close these peaks of the dodecagonal phase. Calculations of T. Ishimasa (private communication) show that for very thin samples of the σ-phase, the peaks corresponding to the two inner rings are very weak, those near the positions of the very strong peaks of Fig. 5.8 are very strong. When the thickness of the sample increases, the weak peaks become much stronger however, whereas the strong peaks get weaker, until the three classes of peaks are of about the same intensity. The dependence of these intensities on sample thickness suggests that this effect is due to multiple scattering. This analogy with the σ-phase supports our hypothesis that multiple scattering is very important also in the dodecagonal case.

In Fig. 5.11 we see that the predicted extinctions are indeed present (i.e. the corresponding peaks are absent). Only in Fig. 5.10 the forbidden odd peaks on the z-axis are not extinct due to multiple scattering effects. This effect can be observed also in decagonal quasicrystals [Be, F]. Interesting to note is also that the layers in Fig. 5.11 which are still present are very weak. The reason is that in the corresponding plane there is none of the very strong peaks of Fig. 5.8, and the intensity remains essentially on the z-axis. May be it will be difficult to observe such a diffraction pattern, and this might be the reason why in [CLK] no such pattern is published, although it would of course be very interesting because of the extinctions.

References

[B] F.P.M. Beenker, *Eindhoven University of Technology Report No. 82-WSK-04,* 1982 (unpublished).

[Ba] P. Bak, *Phys. Rev. Lett.* **56** 861 (1986).

[Be] L. Bendersky, *J. Physique* **47** C3-457 (1986).

[Bes] A.S. Besicovich, *Almost Periodic Functions,* Cambridge University Press: Cambridge 1932.

[BH] P. A. Bancel and P. A. Heiney, *J. Physique* **47** C3-341 (1986).

[Br] H. Brown et al., *Crystallographic Groups of Four-Dimensional Space,*Wiley-Interscience: New York 1978.

[BS] G. Bergman and D.P. Shoemaker, *Acta Cryst.* **7** 857 (1954).

[CLK] H. Chen, D.X. Li and K.H. Kuo, *Phys. Rev. Lett.* **60** 1645 (1988).

[Cox] H. S. M. Coxeter, *Regular Polytopes,* Macmillan: New York 1963

[dB1] N.G. de Bruijn, *Ned. Akad. Wetensch. Proc. Ser. A* **43** 39, 53 (1981).

[dB2] N.G. de Bruijn, *J. Physique* **47** C3-9 (1986).

[DK] M. Duneau and A. Katz, *Phys. Rev. Lett.* **54** 2688 (1985).

[DV] P. DiVicenzo, *J. Physique* **47** C3-237 (1986).

[E1] V. Elser, *Acta Cryst. A* **42** 36 (1986).

[E2] V. Elser, *Phys. Rev. B* **32** 4892 (1985).

[E3] V. Elser, *Phys. Rev. Lett.,* **54** 1730 (1985).

[EH] V. Elser and C. Henley, *Phys. Rev. Lett.* **55** 2883 (1985).

[F] K. K. Fung et al., *Phys. Rev. Lett.* **56** 2060 (1986).

[G1] F. Gähler, *J. Physique* **47** C3-115 (1986).

[G2] F. Gähler, to appear in: *Quasicrystalline Materials,* Ch. Janot and J.M. Dubois (eds.), World Scientific: Singapore 1988.

[Ga] M. Gardner, *Sci. Am.* **236** No. 1, 110 (1977).

[GR] F. Gähler and J. Rhyner, *J. Phys. A: Math. Gen.* **19** 267 (1986).

[HE] C. Henley and V. Elser, *Phil. Mag. B* **53** L59 (1986).

[Hi] P. Hirsch et al., *Electron Microscopy of Thin Crystals,* 2^{nd} ed., Krieger: Malabar 1977.

[Ho] P. M. Horn, W. Malzfeldt, D. P. DiVicenzo, J. Toner and R. Gambino, *Phys. Rev. Lett.* **57** 1444 (1986).

[HT] S. Hendricks and E. Teller, *J. Chem. Phys.* **10** 147 (1942).

[I] T. Ishimasa, *J. Sci. Hiroshima Univ., Ser. A* **45** ,29 (1981).

[IKM] T. Ishimasa, Y. Kitano and Y. Komura, *Phys. Stat. Sol. (a)* **66** 703 (1981).

[INF1] T. Ishimasa, H.-U. Nissen and Y. Fukano, *Phys. Rev. Lett.* **55,** 511 (1985).

[INF2] T. Ishimasa, H.-U. Nissen and Y. Fukano, *Phil. Mag.,* to be published.

[J1] T. Janssen, *J. Physique,* **47** C3-85 (1986).

[J2] T. Janssen, *Acta Cryst. A* **42** 261 (1986).

[J3] T. Janssen, *preprint.*
[K1] P. Kramer, *Z. Naturforsch. A* **40** 775 (1985).
[K2] P. Kramer, *Z. Naturforsch. A* **41** 897 (1986).
[Ka] P.A. Kalugin et al., *JETP Lett.* **41** 145 (1985).
[KD] A. Katz and M. Duneau, *J. Physique* **47** 181 (1986).
[KGR] V. E. Korepin, F. Gähler and J. Rhyner, *Acta Cryst. A, to be published.*
[KN] P. Kramer and R. Neri, *Acta Cryst. A* **40** 580 (1984).
[KNi] L. Kuipers and H. Niederreiter, *Uniform Distribution of Sequences,* Wiley-Interscience: New York 1974.
[LS1] D. Levine and P. J. Steinhardt, *Phys. Rev. Lett.* **53** 2477 (1984).
[LS2] D. Levine and P. J. Steinhardt, *Phys. Rev. B* **34** 596 (1986).
[Lu] T.C. Lubensky et al., *Phys. Rev. Lett.* **57** 1440 (1986).
[LR] L. Levitov and J. Rhyner, *preprint.*
[M1] A.L. Mackay, *Physica* **114A** 609 (1982).
[M2] A.L. Mackay, *Sov. Phys. Crystallogr.* **26** 517 (1981)
[MRW] N.D. Mermin, D.S. Rokhsar and D.C. Wright, *Phys. Rev. Lett.* **58** 2099 (1987).
[NM] N. Niizeki and H. Mitani, *J. Phys. A: Math. Gen.* **20** L405 (1987).
[P] W. Plesken, *Match* **10** 97 (1981).
[Pen] R. Penrose, *Bull. Inst. Math. Appl.* **10** 266 (1974).
R. Penrose, *Math. Intelligencer* **2** 32 (1979).
[PH] W. Plesken and W. Hanrath, *Math. Comp.* **43** 573 (1984).
[Ras] H. Raszillier, *J. Math. Phys.* **25** 1682 (1984).
[RMW] D.S. Rokhsar, N.D. Mermin and D.C. Wright, *Phys. Rev. B* **35** 5487 (1987).
[RWM] D.S. Rokhsar, D.C. Wright and N.D. Mermin, *Acta Cryst. A* **44** 197 (1988).
[S] D. Shechtman et al., *Phys. Rev. Lett.* **53** 1951 (1984).
[SLS] J. E. S. Socolar, T. C. Lubensky and P. J. Steinhardt, *Phys. Rev. B* **34** 3345 (1986).
[SSL] J.E.S. Socolar, P.J. Steinhardt and D. Levine, *Phys. Rev. B* **32** 5547 (1985).
[St] P. Stampfli, *Helv. Phys. Acta* **59** 1260 (1986).
[YW] Q. B. Yang and W. D. Wei, *Phys. Rev. Lett.,* **58** 1020 (1987).
[WCK] N. Wang, H. Chen and K.H. Kuo, *Phys. Rev. Lett.* **59** 1010 (1987).

Dank

Zum Schluss möchte ich mich bei den Professoren und Kollegen in- und ausserhalb des Instituts ganz herzlich bedanken.

Mein besonderer Dank gilt meinem Doktorvater Prof. Jürg Fröhlich, der mir ermöglicht hat, ein Thema eigener Wahl selbständig zu bearbeiten. Seine stete Unterstützung und Ermutigung hat viel zum Gelingen dieser Arbeit beigetragen.

Ganz besonders verpflichtet bin ich auch meinem Freund Jacques Rhyner, der zu gleicher Zeit ein verwandtes Thema bearbeitet hat. Die unzähligen Diskussionen mit ihm haben mir geholfen, noch unausgegorene Ideen zu klären und neue Ideen zu entwickeln. Für diese enge Zusammenarbeit möchte ich mich herzlich bedanken.

Eine grosse Freude ist es auch, meinen Freunden von der Experimentalphysik zu danken. Prof. Hans-Ude Nissen, Dr. T. Ishimasa und Conradin Beeli haben mich in die Geheimnisse des Experiments eingeweiht. Die vielen, langen Diskussionen mit ihnen haben mir sehr geholfen, meine theoretischen Vorstellungen mit der experimentellen Wirklichkeit in Einklang zu bringen. Danken möchte ich Hans-Ude Nissen auch für seinen unermüdlichen Enthusiasmus, der mir immer wieder Mut machte und mich von neuem wieder angestachelt hat, wenn der Weg einmal nicht so klar vorgezeichnet schien.

Besonderer Dank gilt auch Dr. Peter Stampfli, dessen Ideen mich oft inspiriert haben. In einem ausgedehnten Briefwechsel, und – als Höhepunkt – in einem privaten "Quasikristall-Workshop", zu dem er und seine Eltern mich nach Grindelwald eingeladen hatten, haben wir zusammen viel über quasiperiodische Tilings gelernt.

Mein Dank gilt aber auch allen Mitgliedern des Instituts, die hier nicht namentlich erwähnt werden. Sie alle waren immer zu Gesprächen bereit, und haben zusammen eine angenehme, kollegiale Atmosphäre geschaffen, die sehr befruchtend gewirkt hat.

Lebenslauf

26. 7. 1959	geboren in Romanshorn
1966-1972	Primarschule in Güttingen
1972-1978	Sekundarschule in Altnau
1975-1978	Kantonsschule Kreuzlingen Abschluss mit C-Matura
1978-1983	Physikstudium an der ETH Zürich Diplom in theoretischer Physik, Diplomarbeit unter der Leitung von Prof. N. Straumann (Universität Zürich) zum Thema "Wave Fields in Weyl Spaces and Conditions for the Existence of a Preferred Pseudo-Riemannian Structure"
1983-1987	Assistententätigkeit am Institut für Theoretische Physik, ETH Zürich
1987	Doktorarbeit zum Thema "Quasicrystal Structures from the Crystallographic Viewpoint"